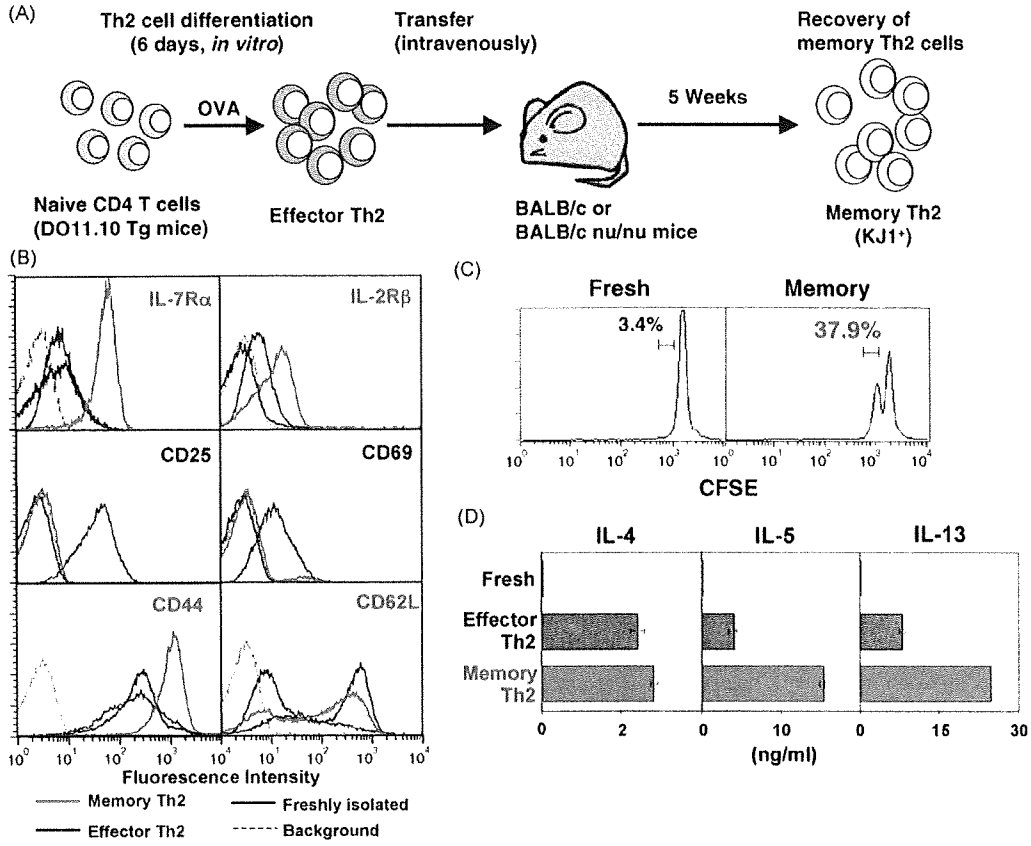

Fig. 1. Generation and phenotypic characterization of OVA-specific memory Th2 cells. (A) The generation of antigen-specific memory Th2 cells by adoptive cell transfer. Splenic CD4 T cells from DO11.10 OVA-specific TCR Tg mice were stimulated with an OVA peptide (Loh15) plus APC under Th2 conditions for 5 days *in vitro*, and then transferred intravenously into normal syngeneic BALB/c or BALB/c *nu/nu* recipient mice. The donor-derived cells (memory Th2 cells) were identified by the staining with anti-clonotypic mAb for the Tg TCR, JK1. (B) Expression profiles of cell surface maker antigens on *in vivo* generated memory Th2 cells. (C) Memory Th2 cells rapidly proliferated in response to the antigen. The cells were labeled with CFSE and stimulated with OVA peptides plus APC for 16 h. The cell division of CFSE-labeled cells was analyzed by flow cytometry. (D) Th2 cyokine production profiles of the *in vivo* generated memory Th2 cells upon *in vitro* antigenic restimulation.

observed when effector Th2 cells are transferred into BALB/c *nu/nu* recipient mice (unpublished observation).

The expression profiles of the surface makers on the *in vivo* generated memory Th2 cells are shown in Fig. 1B. The expression levels of IL-7 receptor (R)α and IL-2 receptor (R)β chains are higher in memory Th2 cells in comparison to those of freshly isolated KJ1$^+$ CD4 T cells from DO11.10 Tg mice or *in vitro* generated effector Th2 cells. The activation markers, CD69 and CD25 (IL-2Rα chain), are not significantly expressed in either memory or naïve populations, whereas effector Th2 cells expressed these makers substantially. The high-level expression of CD44 is observed in the memory Th2 cells. Two subpopulations with high and low expression of CD62L (phenotypically central and effector memory cells, respectively) are observed in memory Th2 cells.

Memory T cells proliferate rapidly in response to a low concentration of antigens in comparison to naïve T cells [14]. *In vivo* generated memory Th2 cells from the spleen were labeled with CFSE *in vitro*, and stimulated with two different doses of OVA peptides and APC for 16 h. Freshly isolated CD4 T cells from DO11.10 Tg mice do not proliferate (3.4%) during the first 16 h after stimulation, whereas substantial numbers of memory Th2 cells (37.9%) divided once in response to the antigenic peptide (Fig. 1C). Similar results are obtained in Th1 cells (unpublished observation).

Cytokine production profiles are also maintained in the *in vivo* generated memory Th2 cells (Fig. 1D). After restimulation with antigenic peptide *in vitro*, the *in vivo* generated memory Th2 cells produced large amounts of Th2 cytokines (IL-4, IL-5 and IL-13) and the levels are equivalent or higher than those of effector Th2 cells.

Taken as a whole, these results indicate that the *in vivo* generated memory Th2 cells possess the phenotypic and functional properties that are typical for memory cells.

3. Molecular basis for the maintenance of memory CD4 T cells

In contrast to CD8 memory T cells, CD4 memory T cells may not require any specific cytokine signals for their homeostatic maintenance [15,16]. Memory CD4 T cells that lack common γ-chain (γc) could survive normally *in vivo* [17]. However, a role for IL-7 in memory CD4 T cells is demonstrated when the TCR-mediated signals are impaired [18]. Therefore, IL-7 may play a role in the regulation of the generation and survival of CD4 memory T cells [18–20]. The γc cytokines such as IL-7, IL-2, and IL-15 transduce signals through the recruitment of Jak1 and Jak3, which phosphorylate STAT5 [21]. The proto-oncogenes Pim1 and Pim2, which are transcriptional targets of STAT5, are preferentially expressed in the central memory T cell subset [22]. In addition, a higher level of STAT5 phosphorylation is induced by IL-2/IL-7-treatment in central memory T cells in comparison to effector memory T cells. These results suggest that central memory T cells are more sensitive to the γc cytokines to be activated and proliferate.

Recently, the upregulation of several target genes (Bim, Gadd45α, p130 proteins and Fas ligand) of the forkhead-family

transcription factor, FOXO3a was reported in CD4+ effector memory T cells [23]. The activity of FOXO3a is suppressed by Akt- and IKK-mediated Ser/Thr-phosphorylation [24,25]. Stimulation via the TCR/CD28 and cytokines activated Akt through the PI3K-dependent signaling pathway and regulated phosphorylation of FOXO3. TCR/CD28-mediated signals induced phosphorylation on Ser315 of FOXO3a, whereas IL-2/IL-7 stimulation results in the phosphorylation on Thr315 [23]. The preferential activation of these cascades in central memory T cells may therefore support the survival of these cells.

The OX40-dependent signaling either from APC or other activated CD4 T cells are reported to be required for the sufficient generation of memory CD4 T cells, at least under Th2 conditions [26,27]. GATA3 is required for the maintenance of Th2 cytokine production [28–30] and chromatin remodeling of the Th2 cytokine gene loci [28]. Memory Th2 cells maintain the Th2 features, such as selective Th2 cytokine production, a high-level expression of GATA3 mRNA and histone modifications of the Th2 cytokine gene loci in an IL-4-independent manner [13]. However, the molecules that control the maintenance of these Th2 features in memory Th2 cells have only recently been identified.

Table 1
Major components of the Polycomb/Trithorax complexes.

Drosophila protein	Protein domains	Mouse protein homologues
Polycomb group		
PC	Chromodomain	M33 (CBX2), CBX4, 6–8
PH	SAM	PHC1–3
PSC	RING	BMI1, Mel18
SCE	RING	RING1A/B
SCM	SAM, MBT, Zinc-finger	SCMH1, 2
E(Z)	SET	EZH1, 2
ESC/ESCL	WD40	EED
SU(Z)12	Zinc-finger	SUZ12
PHO/PHOL	Zinc-finger	YY1
ASX	PHD	ASXL1, 2
SFMBT	SAM, MBT	L3MBTL2, MBTD1
Trithorax group		
TRX	PHD, SET	MLL1, WBP7
ASH1	PHD, SET, BAH	ASH1
ASH2	PHD, SPRY	ASH2L
BRM	SNF2, Bromodomain	SMARCA4
MOR	SWIRM, SAINT	SMARCC1, 2
OSA	BRIGHT	ARID1B

Ref. [33].

4. PcG and TrxG gene products control cellular memory

In general, the gene expression in eukaryotic cells is maintained by epigenetic changes in the chromatin structure [31]. These changes include covalent posttranslational modification of nucleosomal histones, DNA methylation and remodeling of the nucleosome structure [32]. Recent studies provide substantial evidence indicating that PcG and TrxG proteins are key components for the maintenance of chromatin structures. The members of PcG and TrxG family proteins are summarized in Table 1 [33].

The PcG gene products were first identified in *Drosophila melanogaster* as molecules that are required for maintaining proper expression pattern of *homeotic* (*Hox*) genes [34]. The PcG gene is required for the maintenance of the repressed state of its target genes. PcG silencing involves at least two kinds of multimeric heterogenous protein complex, called Polycomb repressive complex 1 (PRC1) and PRC2 (Fig. 2A). The mammalian PRC1 complex has been isolated and identified from Hela cells [35]. The purified complex contains Ring1A/B, HPC1/2/3, HPH1/2, Bmi1 and Mel18. The PRC1 contains Polycomb (Pc) molecule, and the PRC1 is able to bind specifically to the tri-methylated histone H3-K27 via the chromodomain of the Pc molecules [36]. The key component of the mammalian PRC2 complex is the Enhancer of Zeste homolog (Ezh2) having an intrinsic histone methyltransferase activity for histone

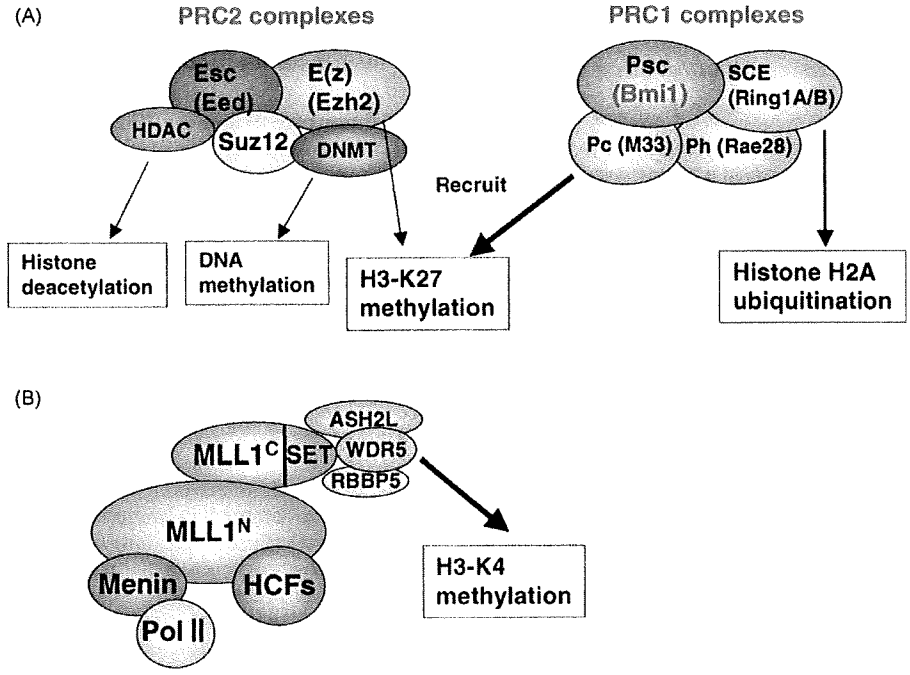

Fig. 2. Schematic representation of PcG and TrxG molecule complexes. (A) PcG proteins form at least two types of multiprotein complexes Polycomb repressive complex 1 (PRC1) and PRC2. E(z) has an intrinsic activity of tri-methylation of histone H3-K27 [51–54]. SCE (Ring 1B) monoubiquitinates histone H2A-K119 [55,56]. The chromodomain of Pc recognizes the tri-methylated histone H3-K27 [36]. PRC2 contains DNMTs (DNA methyl transferases) and HDACs (histone deacetylases). (B) A proposed Trx complex containing MLL1. MLL1 is reported to be associated with ASH2L, RbBP5, WDR5, and Menin [57]. RbBP5 and WDR5 are the WD40 repeat containing protein. The MLL complex has an activity of tri-methylation of histone H3-K4.

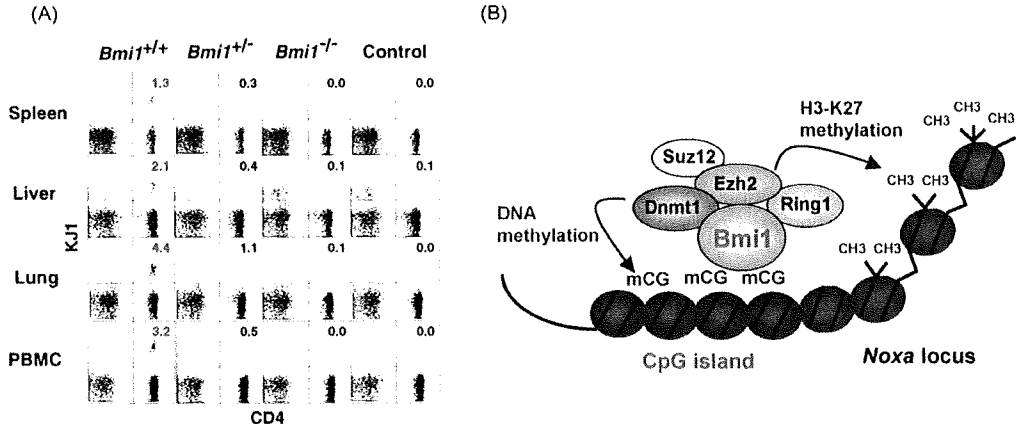

Fig. 3. Bmi1 regulates memory Th2 cell generation via direct binding to the *Noxa* gene. (A) Impaired generation of memory Th2 cells from *Bmi1*$^{-/-}$ effector Th2 cells. *Bmi1*$^{+/+}$, *Bmi1*$^{+/-}$ or *Bmi1*$^{-/-}$ effector Th2 cells with DO11.10 Tg background were intravenously transferred into syngeneic BALB/c mice. Five weeks later, the number of donor-derived KJ1^{+} memory Th2 cells was determined by flow cytometry. (B) A proposed Bmi1 containing PcG complex that regulates directly the expression of *Noxa*. Dnmt1, Ring1, Ezh2, and Suz12 are recruited to the CpG island of the *Noxa* gene locus, and the methylation of genomic DNA and histone H3-K27 of this region was detected [47].

H3-K27. Interestingly, DNA methyltransferase 1 (DNMT1) and histone deacetylases (HDACs) are also components of PRC2, and thus PRC2 appears to be able to negatively regulate the expression of target genes. The mammalian PRC2 complex contains at least two other PcG molecules, namely Suz12 and Eed.

The major role of TrxG gene products in the regulation of the *Hox* gene expression is to prevent PcG gene product-mediated silencing [37,38]. The mammalian homolog of *Drosophila trithorax* (*trx*) gene, *Mixed-Lineage Leukemia 1* (*MLL1*) gene is isolated as a common target of chromosomal translocations observed in human acute leukemias [39–43]. MLL1 forms a multi-component complex containing other TrxG protein, ASH2L (Fig. 2B), and has a histone methyltransferase activity specific for histone H3-K4, a modification typically associated with the transcriptionally active regions of chromatin [44,45].

5. Essential role of Bmi1 in the regulation of memory T cell survival

Memory T cells have several features associated with stem cells, and the similarity of the gene expression pattern between memory T/B cells and long-term hematopoietic stem cells is reported [46]. Similar to hematopoietic stem cells, memory T cells appear to possess the ability to proliferate in response to homeostatic signals. The PcG gene *Bmi1* has recently been implicated in the maintenance of hematopoietic [8,9], neural [10] and cancer stem cells [11]. The role of Bmi1 in the generation and maintenance of memory Th1/Th2 cells was investigated using the memory Th cell generation system stated above [47]. A *Bmi1* gene dose-dependent decrease in the numbers of memory Th2 cells is observed in all tissues tested (spleen, liver, lung, and peripheral blood mononuclear cells; PBMC) (Fig. 3A). Memory Th1 cell generation from *Bmi1*$^{-/-}$ effector Th1 cells is also impaired. This is also observed when they were transferred to lymphopenic BALB/c *nu/nu* mice [47]. These results clearly indicate that Bmi1 expression is required for the generation of memory Th1/Th2 cells.

Bmi1 has been reported to control cell proliferation and stem cell self-renewal by repressing the *Ink4a/Arf* locus [48]. This locus codes for two proteins, p16^{ink4a} and p19^{arf} (Ink4a and Arf), through the use of alternative reading frames. Ink4a is a cyclin D-dependent kinase inhibitor that induces cell cycle arrest following Rb activation. Arf induces p53 activation and p53-mediated cell death [49]. Although the increased expression of mRNA is observed in the *Ink4a/Arf* in *Bmi1*$^{-/-}$ memory Th2 cells, the deletion of the *Ink4a* and *Arf* genes failed to restore memory Th2 cell generation in *Bmi1*$^{-/-}$ [47]. Among the pro-apoptotic genes (*Bax, Puma, Noxa, Bim, Bad, Fas* and *Fas ligand*) that increased in *Bmi1*$^{-/-}$ Th2 cells, the level of *Noxa* mRNA remained high in *Bmi1*$^{-/-}$/*Ink4a*$^{-/-}$/*Arf*$^{-/-}$ Th2 cells. Noxa is a member of BH3-only protein family that initiates programmed cell death in various cells including lymphocytes. Bmi1 binds to the CpG islands at *Noxa* gene and suppresses the expression of *Noxa* through the maintenance of H3-K27 histone methylation. The other PcG family proteins, such as Ring1B and Suz12 also bind to the Noxa gene locus (Fig. 3B). In addition, Bmi1-dependent recruitment of Dnmt1 at the *Noxa* gene locus is observed. Furthermore, Noxa-deletion significantly rescued the effects of Bmi1-deficiency on memory Th2 cell generation. Mel-18, Mph1/Rae28, Ring1B and M33 are also found to be involved in the regulation of memory Th2 cell generation (unpublished observation). Therefore, Bmi1 containing PcG complex regulates memory Th cell survival at least in part through the regulation of *Noxa* gene expression.

6. Maintenance of memory Th2 cell function regulated by TrxG molecule, MLL1

Some of the effector Th cells are maintained as memory Th cells for a long time *in vivo* [4]. In memory Th2 cells, GATA3 is required for the maintenance of Th2 cytokine production [28–30] and chromatin remodeling of the Th2 cytokine gene loci [28]. Memory Th2 cells maintain the Th2 features, such as selective Th2 cytokine production upon recall stimulation, high-level expression of GATA3 mRNA and histone modifications of the Th2 cytokine gene loci in an IL-4-independent manner [13]. To maintain a high-level expression of GATA3 and subsequent Th2 cytokine production, MLL1, a member of TrxG protein, has been found to play a crucial role [50]. MLL is involved in one of the nuclear regulatory mechanism that establishes an epigenetic transcriptional memory system [12]. MLL1 forms a multi-component complex and mediates its epigenetic transcriptional effector functions via the SET domain-dependent histone methyltransferase activity [44,45] (Fig. 2B). MLL1 specifically methylates lysine 4 (K4) present on histone H3, a modification typically associated with the transcriptionally active regions of chromatin. A substantial decrease in the transcription of GATA3 accompanied by decreased methylation levels of H3-K4 at the GATA3 gene locus are detected in MLL1-knockdown Th2 cell lines and in *in vivo* generated memory Th2 cells with an *MLL1* heterozygous background [50]. MLL1 appears to regulate the memory Th2 responses through the control of chromatin remodeling at the

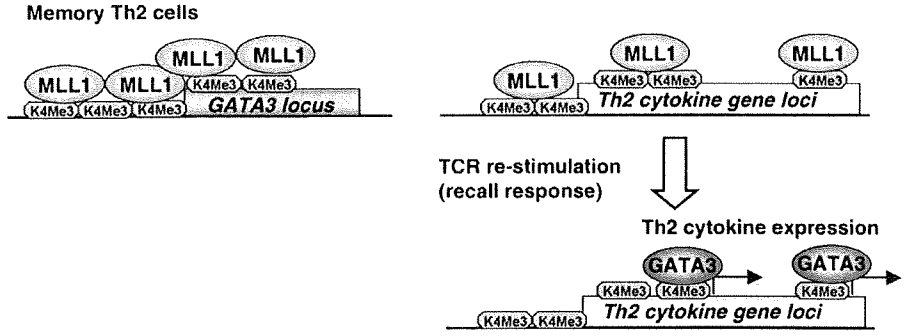

Fig. 4. MLL controls the maintenance of open chromatin of the GATA3 and Th2 cytokine gene loci in memory Th2 cells. In memory Th2 cells, MLL binds to the GATA3 gene locus and Th2 cytokine gene loci to maintain the open chromatin of these loci accompanied with histone H3-K4 methylation. Upon TCR restimulation during recall responses, GATA3 plays an important role in the transcription of Th2 cytokine genes. In memory Th2 cells, GATA3 does not play a major role in the regulation of chromatin status, but still plays an important role as a transcription factor for the Th2 cytokine gene.

GATA3 locus and subsequent GATA3 expression in Th2 cells (Fig. 4). In addition to the GATA3 gene locus, MLL1 is also found to be involved in the maintenance of activated chromatin status at the Th2 cytokine gene loci (Fig. 4). The direct binding of MLL1 at specific regions on the IL-4 and IL-13 gene loci as well as GATA3 gene locus is detected. Th2 cytokine production was severely reduced in *MLL1*-knockdown Th2 cell lines and *MLL1* heterozygous memory Th2 cells accompanied by decreased levels of H3-K9/14 acetylation and H3-K4 methylation. The antigen-induced allergic airway inflammatory responses *in vivo* are also compromised in $MLL1^{+/-}$ memory Th2 mice, thus suggesting a physiological role for MLL1 in the regulation of allergic reactions. Therefore, the maintenance of transcriptional expression of GATA3 in established Th2 cells including memory Th2 cells is epigenetically regulated by TrxG molecule MLL1.

7. Concluding remarks

In the past a few years, new insights into the molecular requirement for the epigenetic regulation of the function of CD4 T cells have emerged. PcG and TrxG gene products counteract each other in the epigenetic function during the development in *Drosophila* and mammals. In contrast, PcG and TrxG gene products have been found to regulate different processes during the generation and the maintenance of memory CD4 T cells. The mode of regulation by PcG and TrxG is also distinct. PcG and TrxG complexes are heterogenous and the components in the complexes appear to be different in different cell types and also in the different developmental stages. Therefore, the analyses of the precise molecular actions of a particular complex formed in a specific process during the initiation and the maintenance of functional memory Th1/Th2 cell would be most important. Moreover, similar to Th1/Th2 cells, further investigation of the regulation by RcG and TrxG molecules in other functionally distinct CD4 T cell subsets, such as Th17, follicular helper T (Tfh), regulatory T (Treg) and Th9 would also be intriguing.

Acknowledgements

This work was supported by Global COE Program (Global Center for Education and Research in Immune System Regulation and Treatment), MEXT (Japan), and by grants from the Ministry of Education, Culture, Sports, Science and Technology (Japan) (Grants-in-Aid: for Scientific Research on Priority Areas #17016010, #20060003; Scientific Research (B) #17390139, Scientific Research (C) #20590485, Exploratory Research #19659121: Special Coordination Funds for Promoting Science and Technology, and: Cancer Translational Research Project), the Ministry of Health, Labor and Welfare (Japan).

References

[1] Marrack P, Kappler J. Control of T cell viability. Annu Rev Immunol 2004;22:765–87.
[2] Stockinger B, Kassiotis G, Bourgeois C. CD4 T-cell memory. Semin Immunol 2004;16:295–303.
[3] Dutton RW, Bradley LM, Swain SL. T cell memory. Annu Rev Immunol 1998;16:201–23.
[4] Sprent J, Surh CD. T cell memory. Annu Rev Immunol 2002;20:551–79.
[5] Nakayama T, Yamashita M. Initiation and maintenance of Th2 cell identity. Curr Opin Immunol 2008;20:265–71.
[6] Satijn DP, Otte AP. Polycomb group protein complexes: do different complexes regulate distinct target genes? Biochim Biophys Acta 1999;1447:1–16.
[7] van Lohuizen M. The trithorax-group and polycomb-group chromatin modifiers: implications for disease. Curr Opin Genet Dev 1999;9:355–61.
[8] Park IK, Qian D, Kiel M, Becker MW, Pihalja M, Weissman IL, et al. Bmi-1 is required for maintenance of adult self-renewing haematopoietic stem cells. Nature 2003;423:302–5.
[9] Iwama A, Oguro H, Negishi M, Kato Y, Morita Y, Tsukui H, et al. Enhanced self-renewal of hematopoietic stem cells mediated by the polycomb gene product Bmi-1. Immunity 2004;21:843–51.
[10] Molofsky AV, Pardal R, Iwashita T, Park IK, Clarke MF, Morrison SJ. *Bmi-1* dependence distinguishes neural stem cell self-renewal from progenitor proliferation. Nature 2003;425:962–7.
[11] Lessard J, Sauvageau G. *Bmi-1* determines the proliferative capacity of normal and leukaemic stem cells. Nature 2003;423:255–60.
[12] Francis NJ, Kingston RE. Mechanisms of transcriptional memory. Nat Rev Mol Cell Biol 2001;2:409–21.
[13] Yamashita M, Shinnakasu R, Nigo Y, Kimura M, Hasegawa A, Taniguchi M, et al. Interleukin (IL)-4-independent maintenance of histone modification of the IL-4 gene loci in memory Th2 cells. J Biol Chem 2004;279:39454–64.
[14] Rogers PR, Dubey C, Swain SL. Qualitative changes accompany memory T cell generation: faster, more effective responses at lower doses of antigen. J Immunol 2000;164:2338–46.
[15] Jameson SC. Maintaining the norm: T-cell homeostasis. Nat Rev Immunol 2002;2:547–56.
[16] Schluns KS, Lefrancois L. Cytokine control of memory T-cell development and survival. Nat Rev Immunol 2003;3:269–79.
[17] Lantz O, Grandjean I, Matzinger P, Di Santo JP. γ Chain required for naive $CD4^+$ T cell survival but not for antigen proliferation. Nat Immunol 2000;1:54–8.
[18] Seddon B, Tomlinson P, Zamoyska R. Interleukin 7 and T cell receptor signals regulate homeostasis of CD4 memory cells. Nat Immunol 2003;4:680–6.
[19] Kondrack RM, Harbertson J, Tan JT, McBreen ME, Surh CD, Bradley LM. Interleukin 7 regulates the survival and generation of memory CD4 cells. J Exp Med 2003;198:1797–806.
[20] Li J, Huston G, Swain SL. IL-7 promotes the transition of CD4 effectors to persistent memory cells. J Exp Med 2003;198:1807–15.
[21] Paukku K, Silvennoinen O. STATs as critical mediators of signal transduction and transcription: lessons learned from STAT5. Cytokine Growth Factor Rev 2004;15:435–55.
[22] White E. The pims and outs of survival signaling: role for the Pim-2 protein kinase in the suppression of apoptosis by cytokines. Genes Dev 2003;17:1813–6.
[23] Riou C, Yassine-Diab B, Van grevenynghe J, Somogyi R, Greller LD, Gagnon D, et al. Convergence of TCR and cytokine signaling leads to FOXO3a phosphorylation and drives the survival of CD4+ central memory T cells. J Exp Med 2007;204:79–91.
[24] Datta SR, Brunet A, Greenberg ME. Cellular survival: a play in three Akts. Genes Dev 1999;13:2905–27.
[25] Hu MC, Lee DF, Xia W, Golfman LS, Ou-Yang F, Yang JY, et al. IkappaB kinase promotes tumorigenesis through inhibition of forkhead FOXO3a. Cell 2004;117:225–37.

[26] Soroosh P, Ine S, Sugamura K, Ishii N. OX40–OX40 ligand interaction through T cell–T cell contact contributes to CD4 T cell longevity. J Immunol 2006;176:5975–87.
[27] Weinberg AD, Evans DE, Thalhofer C, Shi T, Prell RA. The generation of T cell memory: a review describing the molecular and cellular events following OX40 (CD134) engagement. J Leukoc Biol 2004;75:962–72.
[28] Yamashita M, Ukai-Tadenuma M, Miyamoto T, Sugaya K, Hosokawa H, Hasegawa A, et al. Essential role of GATA3 for the maintenance of type 2 helper T (Th2) cytokine production and chromatin remodeling at the Th2 cytokine gene loci. J Biol Chem 2004;279:26983–90.
[29] Pai SY, Truitt ML, Ho IC. GATA-3 deficiency abrogates the development and maintenance of T helper type 2 cells. Proc Natl Acad Sci USA 2004;101:1993–8.
[30] Zhu J, Min B, Hu-Li J, Watson CJ, Grinberg A, Wang Q, et al. Conditional deletion of *Gata3* shows its essential function in T_H1–T_H2 responses. Nat Immunol 2004;5:1157–65.
[31] Horn PJ, Peterson CL. Molecular biology. Chromatin higher order folding—wrapping up transcription. Science 2002;297:1824–7.
[32] Jenuwein T, Allis CD. Translating the histone code. Science 2001;293:1074–80.
[33] Schwartz YB, Pirrotta V. Polycomb silencing mechanisms and the management of genomic programmes. Nat Rev Genet 2007;8:9–22.
[34] Lewis EB. A gene complex controlling segmentation in *Drosophila*. Nature 1978;276:565–70.
[35] Levine SS, Weiss A, Erdjument-Bromage H, Shao Z, Tempst P, Kingston RE. The core of the polycomb repressive complex is compositionally and functionally conserved in flies and humans. Mol Cell Biol 2002;22:6070–8.
[36] Fischle W, Wang Y, Jacobs SA, Kim Y, Allis CD, Khorasanizadeh S. Molecular basis for the discrimination of repressive methyl-lysine marks in histone H3 by Polycomb and HP1 chromodomains. Genes Dev 2003;17:1870–81.
[37] Poux S, Horard B, Sigrist CJ, Pirrotta V. The *Drosophila trithorax* protein is a coactivator required to prevent re-establishment of polycomb silencing. Development 2002;129:2483–93.
[38] Klymenko T, Muller J. The histone methyltransferases Trithorax and Ash1 prevent transcriptional silencing by Polycomb group proteins. EMBO Rep 2004;5:373–7.
[39] Ziemin-van der Poel S, McCabe NR, Gill HJ, Espinosa III R, Patel Y, Harden A, et al. Identification of a gene, *MLL*, that spans the breakpoint in 11q23 translocations associated with human leukemias. Proc Natl Acad Sci USA 1991;88:10735–9.
[40] Gu Y, Nakamura T, Alder H, Prasad R, Canaani O, Cimino G, et al. The t(4;11) chromosome translocation of human acute leukemias fuses the ALL-1 gene, related to *Drosophila trithorax*, to the AF-4 gene. Cell 1992;71:701–8.
[41] Tkachuk DC, Kohler S, Cleary ML. Involvement of a homolog of *Drosophila trithorax* by 11q23 chromosomal translocations in acute leukemias. Cell 1992;71:691–700.
[42] Thirman MJ, Gill HJ, Burnett RC, Mbangkollo D, McCabe NR, Kobayashi H, et al. Rearrangement of the MLL gene in acute lymphoblastic and acute myeloid leukemias with 11q23 chromosomal translocations. N Engl J Med 1993;329:909–14.
[43] Popovic R, Zeleznik-Le NJ. MLL: how complex does it get? J Cell Biochem 2005;95:234–42.
[44] Milne TA, Briggs SD, Brock HW, Martin ME, Gibbs D, Allis CD, et al. MLL targets SET domain methyltransferase activity to *Hox* gene promoters. Mol Cell 2002;10:1107–17.
[45] Nakamura T, Mori T, Tada S, Krajewski W, Rozovskaia T, Wassell R, et al. ALL-1 is a histone methyltransferase that assembles a supercomplex of proteins involved in transcriptional regulation. Mol Cell 2002;10:1119–28.
[46] Luckey CJ, Bhattacharya D, Goldrath AW, Weissman IL, Benoist C, Mathis D. Memory T and memory B cells share a transcriptional program of self-renewal with long-term hematopoietic stem cells. Proc Natl Acad Sci USA 2006;103:3304–9.
[47] Yamashita M, Kuwahara M, Suzuki A, Hirahara K, Shinnaksu R, Hosokawa H, et al. Bmi1 regulates memory CD4 T cell survival via repression of the Noxa gene. J Exp Med 2008;205:1109–20.
[48] Jacobs JJ, Kieboom K, Marino S, DePinho RA, van Lohuizen M. The oncogene and Polycomb-group gene *bmi-1* regulates cell proliferation and senescence through the *ink4a* locus. Nature 1999;397:164–8.
[49] Lowe SW, Sherr CJ. Tumor suppression by *Ink4a–Arf*: progress and puzzles. Curr Opin Genet Dev 2003;13:77–83.
[50] Yamashita M, Hirahara K, Shinnakasu R, Hosokawa H, Norikane S, Kimura MY, et al. Crucial role of MLL for the maintenance of memory T helper type 2 cell responses. Immunity 2006;24:611–22.
[51] Czermin B, Melfi R, McCabe D, Seitz V, Imhof A, Pirrotta V. *Drosophila* enhancer of Zeste/ESC complexes have a histone H3 methyltransferase activity that marks chromosomal Polycomb sites. Cell 2002;111:185–96.
[52] Muller J, Hart CM, Francis NJ, Vargas ML, Sengupta A, Wild B, et al. Histone methyltransferase activity of a *Drosophila* Polycomb group repressor complex. Cell 2002;111:197–208.
[53] Cao R, Wang L, Wang H, Xia L, Erdjument-Bromage H, Tempst P, et al. Role of histone H3 lysine 27 methylation in Polycomb-group silencing. Science 2002;298:1039–43.
[54] Kuzmichev A, Nishioka K, Erdjument-Bromage H, Tempst P, Reinberg D. Histone methyltransferase activity associated with a human multiprotein complex containing the Enhancer of Zeste protein. Genes Dev 2002;16:2893–905.
[55] Wang H, Wang L, Erdjument-Bromage H, Vidal M, Tempst P, Jones RS, et al. Role of histone H2A ubiquitination in Polycomb silencing. Nature 2004;431:873–8.
[56] de Napoles M, Mermoud JE, Wakao R, Tang YA, Endoh M, Appanah R, et al. Polycomb group proteins Ring1A/B link ubiquitylation of histone H2A to heritable gene silencing and X inactivation. Dev Cell 2004;7:663–76.
[57] Yokoyama A, Wang Z, Wysocka J, Sanyal M, Aufiero DJ, Kitabayashi I, et al. Leukemia proto-oncoprotein MLL forms a SET1-like histone methyltransferase complex with menin to regulate *Hox* gene expression. Mol Cell Biol 2004;24:5639–49.

Enhanced Th2 Cell Differentiation and Allergen-Induced Airway Inflammation in *Zfp35*-Deficient Mice[1]

Masayuki Kitajima,* Chiaki Iwamura,* Takako Miki-Hosokawa,* Kenta Shinoda,* Yusuke Endo,* Yukiko Watanabe,* Ryo Shinnakasu,* Hiroyuki Hosokawa,* Kahoko Hashimoto,† Shinichiro Motohashi,* Haruhiko Koseki,‡ Osamu Ohara,§ Masakatsu Yamashita,* and Toshinori Nakayama[2]*

Studies of human asthma and of animal models of allergic airway inflammation revealed a crucial role for Th2 cells in the pathogenesis of allergic asthma. Kruppel-type zinc finger proteins are the largest family of a regulatory transcription factor for cellular development and function. Zinc finger protein (Zfp) 35 is an 18-zinc finger motif-containing Kruppel-type zinc finger protein, while its function remains largely unknown. The aim of this study was to clarify the role of Zfp35 in the pathogenesis of Th2-dependent allergic inflammation, such as allergic asthma. We examined airway eosinophilic inflammation and hyperresponsiveness in two mouse models, which use our newly generated Zfp35-deficient (*Zfp35*$^{-/-}$) mice and adoptive transfer of cells. In *Zfp35*$^{-/-}$ mice, Th2 cell differentiation, Th2 cytokine production, eosinophilic inflammation, and airway hyperresponsiveness were substantially enhanced. Furthermore, adoptive transfer of Ag-sensitized *Zfp35*$^{-/-}$ CD4 T cells into the asthmatic mice resulted in enhanced airway inflammation and airway hyperresponsiveness. These results indicate that Zfp35 controls Th2 cell differentiation, allergic airway inflammation, and airway hyperresponsiveness in a negative manner. Thus, Zfp35 may control Th2-dependent diseases, such as allergic asthma. *The Journal of Immunology,* 2009, 183: 5388–5396.

Asthma is a chronic inflammatory disease of the lower airways that causes airway hyperresponsiveness (AHR)[3] to a wide variety of specific and nonspecific stimuli (1, 2). Acute allergic asthma represents airway inflammation predominated by eosinophils, hypersecretion of mucus, and AHR. The involvement of Th2 cells in the pathogenesis of allergic asthma has been well recognized through the studies of human asthma as well as of animal models of allergic airway inflammation (3–9).

It is well recognized that CD4$^+$ effector Th cells are categorized into three subsets, Th1, Th2, and Th17 cell subsets. Th1 cells produce IFN-γ and direct cell-mediated immunity against intracellular pathogens. Th2 cells produce IL-4, IL-5, and IL-13 and are involved in humoral immunity and allergic reactions. Th17 cells, a recently identified population (10), produce IL-17 and play a critical role in the pathogenesis of autoimmune diseases (11–13). Several transcription factors that control the differentiation of these Th subsets have been identified. Among them, a zinc finger transcription factor GATA3 appears to be a key transcription factor for Th2 cell differentiation (14, 15), T-bet for Th1 (16), and Retinoid-related orphan receptor γ t for Th17 cell differentiation (17).

Transcription factors play critical roles in a variety of cellular processes, such as differentiation, proliferation, cell death, and survival through specific induction/repression of the target genes (18–20). The Cys^{2}His^2 (C_2H_2)-type zinc finger proteins (Zfps) are one of the well-defined eukaryotic DNA-binding proteins, and ~700 genes existed in the human genome (21–23). The C_2H_2-type zinc finger motif is composed of 21 aa with a consensus sequence of $CX_2CX_3FX_5LX_2HX_3H$ and contains two conserved cysteine and histamine residues that coordinate a zinc ion and fold the domain into a finger-like structure (24, 25). The investigation of C_2H_2-type Zfps suggested their unique and specific roles in the regulation of lymphocyte development. For example, Egr-3, Zfp608, Th-POK, and Gfi-1 are shown to be involved in the differentiation of T cells (26–29). We have recently reported that Schnurri-2 plays a crucial role in the control of Th2 cell differentiation by regulating NF-κB functions (30, 31). In particular, Zfps that possess many zinc finger motifs, such as PLZF, SKAT-2, ZEB, and ZNF304 (these have 9, 14, 7, and 13 zinc finger motifs, respectively), control the IL-4 production from either CD4 T or NKT cells (32–35).

We selected Zfp35 (also known as znf271) in a subtraction analysis where a relatively increased expression of Zfp35 was detected in IL-4^{low}-producing cells in comparison to IL-4^{high}-producing cells in in vitro-generated Th2 cells. Zfp35 belongs

*Department of Immunology, Graduate School of Medicine, Chiba University, Chiba, Japan; †Department of Life and Environmental Sciences and High Technology Research Center, Chiba Institute of Technology, Naraschino, Tsudanuma, Chiba, Japan; and ‡Laboratory for Developmental Genetics and §Laboratory for Immunogenomics, RIKEN Research Center for Allergy and Immunology, Yokohama, Japan

Received for publication December 11, 2008. Accepted for publication August 16, 2009.

The costs of publication of this article were defrayed in part by the payment of page charges. This article must therefore be hereby marked *advertisement* in accordance with 18 U.S.C. Section 1734 solely to indicate this fact.

[1] This work was supported by the Global Center for Education Program (Global Center for Education and Research in Immune System Regulation and Treatment), Monbukagakusho (Japan), and by grants from the Ministry of Education, Culture, Sports, Science and Technology (Japan) (Grants-in-Aid for Scientific Research on Priority Areas no. 17016010 and no. 20060003; Scientific Research (B) no. 21390147, Scientific Research (C) no. 21591808 and no. 20590485, and Young Scientists (B) no. 20790367; and Start-up no. 20890038: Cancer Translational Research Project), the Ministry of Health, Labor and Welfare (Japan), and The Japan Health Science Foundation, Kanae Foundation, and Uehara Memorial Foundation.

[2] Address correspondence and reprint requests to Dr. Toshinori Nakayama, Department of Immunology, Graduate School of Medicine, Chiba University, 1-8-1 Inohana, Chuo-ku, Chiba 260-8670, Japan. E-mail address: tnakayama@faculty.chiba-u.jp

[3] Abbreviations used in this paper: AHR, airway hyperresponsiveness; BAL, bronchoalveolar lavage; EPO, eosinophil peroxidase; Zfp, zinc finger protein; Tg, transgenic; RL, lung resistance.

Copyright © 2009 by The American Association of Immunologists, Inc. 0022-1767/09/$2.00

www.jimmunol.org/cgi/doi/10.4049/jimmunol.0804155

Downloaded from www.jimmunol.org on February 23, 2010

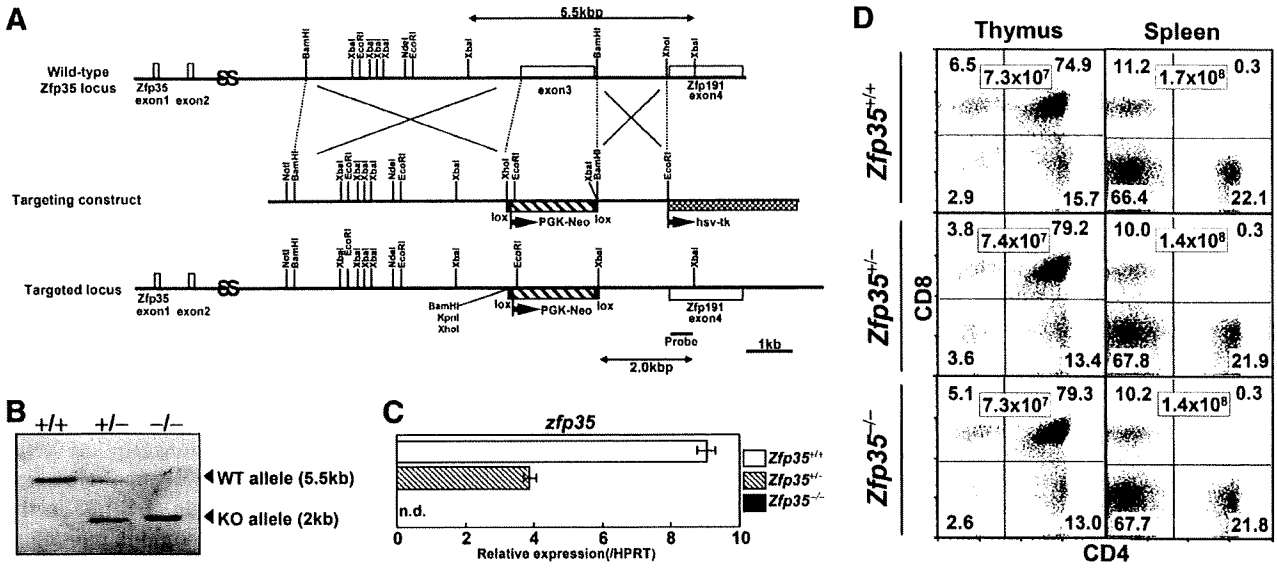

FIGURE 1. Targeted disruption of mouse *Zfp35* gene. *A*, Schematic representation of the *Zfp35* gene, the targeting vector, and the predicted disrupted gene. The probes used for Southern blot analyses are shown along with the predicted sizes of the hybridizing fragments. The open boxes represent translated exons, respectively. *B*, Southern blot analysis of genomic DNA extracted from the tails of wild-type (+/+), *Zfp35*$^{+/-}$ (+/−), and *Zfp35*$^{-/-}$ (−/−) mice. Genomic DNA digested with *XbaI* was hybridized with the probe to yield 5.5- and 2.0-kb bands; these represented the wild-type (WT) and knockout (KO) alleles, respectively. *C*, RNAs were prepared from fresh splenic CD4$^+$ T cells of wild-type (+/+), *Zfp35*$^{+/-}$ (+/−), and *Zfp35*$^{-/-}$ (−/−) mice, and then expression levels of *Zfp35* were determined by the RT-PCR method. Three independent experiments were performed with similar results. n.d., Not detected. *D*, Representative CD4/CD8 profiles of thymocytes and splenocytes of *Zfp35*$^{-/-}$ mice with a BALB/c background. Representative yields of thymocytes and splenocytes are shown in the box.

to C_2H_2-type Zfp family and contains 18 continuous typical C_2H_2 zinc fingers in its C-terminal and contains one acidic region with a numbers of glutamic and aspartic acid domain in its N terminus (36). A human homolog of Zfp35, ZNF^{EB}, was identified in EBV-positive B cells and shows ~79% homology at the amino acid level compared with mice (37). The rat homolog Zfp239 was identified in the cDNA library of the spleen by the Mammalian Gene Collection Program and shows ~84% homology at the amino acid level compared with mice (38). However, the physiological function of Zfp35 and homologs in the immune system has not been investigated.

In this study, we have established Zfp35-deficient (*Zfp35*$^{-/-}$) mice with either a BALB/c or a C57BL/6 background and investigated the role of Zfp35 in Th1/Th2 cell differentiation and also in the pathogenesis of Th2-dependent allergic airway inflammation. Our results indicate that Zfp35 negatively regulates Th2 cell differentiation and Th2-driven airway allergic inflammation.

Materials and Methods

Mice

We have newly established *Zfp35*$^{-/-}$ mice and were backcrossed to either BALB/c or C57BL/6 10 times. *Zfp35*$^{-/-}$ × DO11.10-transgenic (Tg) (an anti-OVA-specific TCR-$\alpha\beta$ Tg) mice (39) were used at 6–8 wk old. BALB/c and C57BL/6 mice were purchased from CLEA Japan. All mice used in this study were maintained under specific pathogen-free conditions. Animal care was conducted in accordance with the guidelines of Chiba University.

Cell purification

Splenic CD4 T cells were purified by using magnetic beads and an AutoMACS Sorter (Miltenyi Biotec) yielding a purity of >98%. Where indicated, splenic CD4 T cells with naive phenotype (CD44^{low}) and eosinophils in the bronchoalveolar lavage (BAL) fluid were isolated on a FACSAria cell sorter (BD Biosciences), yielding a purity of >98% as previously described (40). The lung mononuclear cells were isolated as described previously (41).

In vitro Th1/Th2 cell differentiation cultures

Naive splenic CD4 T cells were stimulated with 3 μg/ml immobilized ant-TCR-β mAb (H57-597) in the presence of 25 U/ml IL-2 and 1–100 U/ml IL-4 as described previously (42). For Th1 cell differentiation, naive splenic CD4 T cells were stimulated with 3 μg/ml immobilized anti-TCR-β mAb (H57-597) in the presence of 25 U/ml IL-2, IL-12, and anti-IL-4 mAb. In brief, 1.5 × 10^4 sorted DO11.10 Tg CD44^{low} CD4 T cells were stimulated with antigenic OVA peptide (Loh15, $OVA_{323-339}$, 0.1 μM) and 10^5 irradiated (3500 rad) normal BALB/c splenocytes. Appropriate cytokines and anti-cytokine Abs were added in Th1/Th2 cell differentiation cultures as described previously (40). In typical DO11.10 Tg T cell cultures, Th2 cell-skewed (IL-4 with anti-IL-12 mAb and anti-IFN-γ mAb) and Th1 cell-skewed (IL-12 with anti-IL-4 mAb) conditions were used.

ELISA for the measurement of cytokine concentration

The production of IL-2, IL-4, IL-5, IL-10, and IFN-γ were measured by ELISA as described elsewhere(43). The production of IL-13 was measured by a mouse IL-13 ELISA kit (R&D Systems) according to the manufacturer's protocol.

Immunofluorescent staining and flow cytometry analysis

In general, one million cells were stained with Abs as indicated according to a standard method (44, 45).

Quantitative RT-PCR

Quantitative RT-PCR was performed as described previously using an Applied Biosystems PRISM 7500 Sequence Detection System under standard conditions (46, 47). The primers for TaqMan probes for the detection of Zfp35 (exons 2 and 3), muc5ac, gob5, IL-4, IL-5, IL-13, eosinophil peroxidase (EPO), and *HPRT* were purchased from Applied Biosystems.

Collection and analysis of BAL fluid

One day after the last challenge with OVA, BAL was prepared as previously described (48). Total BAL fluid was collected and cells in 100-μl aliquots were counted. One hundred thousand viable BAL cells were cytocentrifuged onto slides by a Cytospin 3 (Shandon) and stained with May-Grünwald-Giemsa solution (Merck) as described elsewhere (49). Five hundred leukocytes were counted on each slide. Cell types were identified

Downloaded from www.jimmunol.org on February 23, 2010

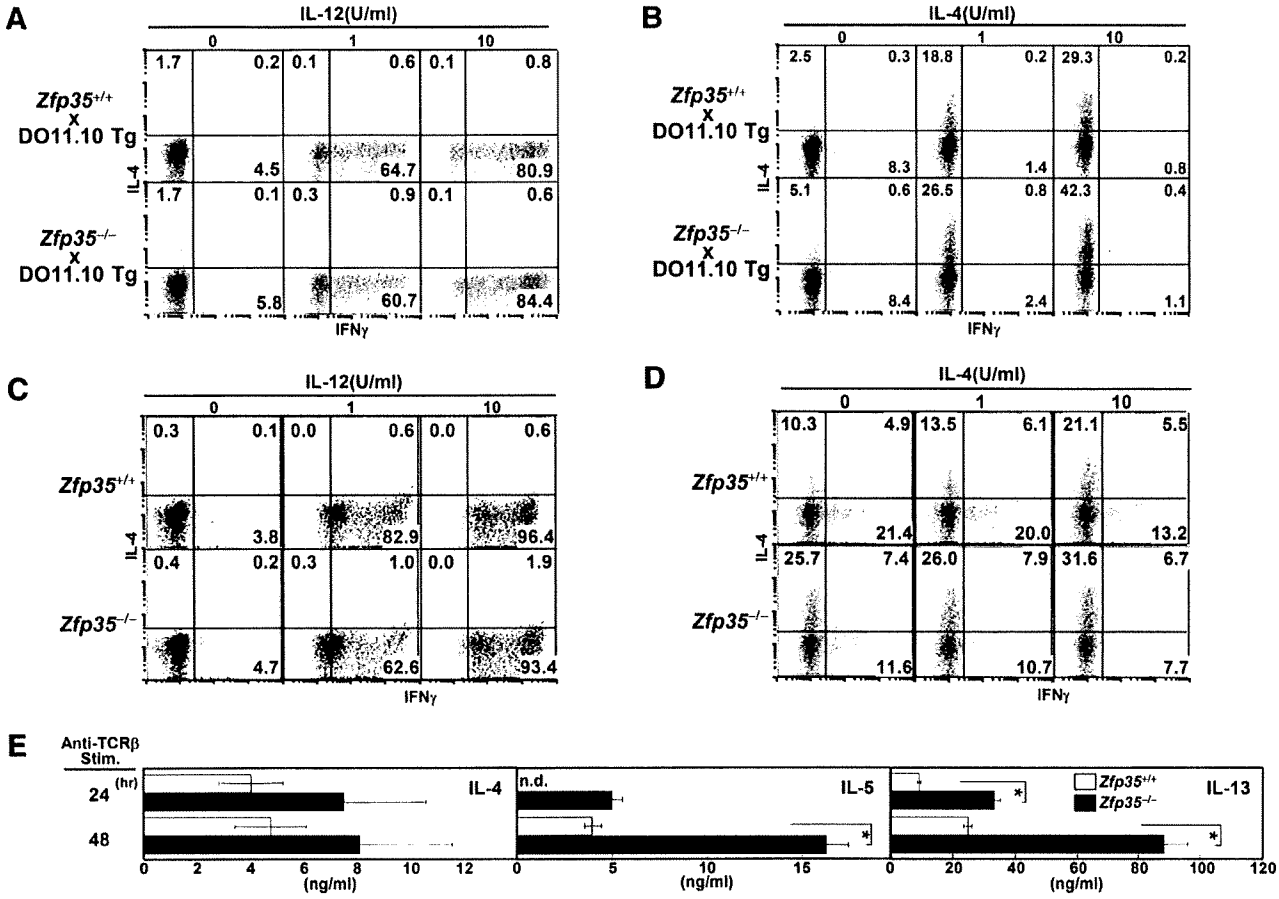

FIGURE 2. Enhanced Th2 cell differentiation in *Zfp35*$^{-/-}$ CD4 T cells. *A* and *B*, The ability to differentiation into Th1/Th2 cells from *Zfp35*$^{-/-}$ × DO 11.10 Tg mice was assessed. The results are representative of five experiments. *C* and *D*, Naive (CD44^{low}) CD4 T cells from *Zfp35*$^{-/-}$ mice were purified by cell sorting and stimulated with immobilized anti-TCR-β mAb (3 μg/ml) under Th1/2 conditions for 5 days. The results are representative of five experiments. *E*, A fraction of the same differentiated cell cultures used in *B* were restimulated with anti-TCR-β mAb for the indicated times. The mean cytokine concentration is shown with SDs. Three independent experiments were performed with similar results. n.d., Not detected.

using morphological criteria. The percentages of each cell type were calculated. Cytokines levels in the BAL fluid were measured 6 h after the last OVA challenges.

Immunization, challenge, and CD4 T cell transfer

Mice were immunized with 1 mg of OVA in alum on day 0. They were challenged on days 7 and 9 intranasally with 100 μg of OVA in 30 μl of saline under anesthesia as previously described (50). Splenic CD4 T cells from OVA-immunized wild-type or *zfp35*-deficient BALB/c mice on day 10 were isolated by the panning method as previously described (40). Prepared CD4 T cells (1.5×10^7 cells) were i.v. transferred into wild-type BALB/c mice. Transferred mice were challenged on days 11 and 13 intranasally as above.

OVA inhalation and analysis of airway inflammation

AHR responses were assessed by methacholine-induced airflow obstruction in conscious mice placed in a whole-body plethysmograph (Buxco Electronics) as described previously (50). Airway function was also assessed by measuring the changes in lung resistance (RL) and dynamic compliance in response to increasing doses of inhaled methacholine, as described previously (51, 52).

Analysis of lung histology

The lung samples taken on day 11 were sectioned, stained with H&E reagents, periodic acid-Schiff reagents, and Luna reagents as described previously (50).

Statistical analysis

The significance between two groups was determined by two-tailed Student's *t* test. Mann-Whitney *U* tests were used to determine the level of difference in the degree of AHR.

Results

Establishment of knockout mice for Zfp35 *gene*

To functional analyze the Zfp35, the targeting strategy to inactivate *Zfp35* is described in Fig. 1. Germline chimeras and mice heterozygous for the mutated *Zfp35* gene were generated as described in *Materials and Methods*. Southern blot analysis with the 3′ external probe confirmed the correct recombination (Fig. 1*B*). We also assessed the mRNA expression of *Zfp35* in freshly prepared splenic CD4 T cells from BALB/c and Zfp35-deficient mice. Real-time RT-PCR analysis demonstrated that there was no detectable *Zfp35* transcript in Zfp35-deficient splenic CD4 T cells (Fig. 1*C*).

Phenotypic and function characterization of CD4 T cells in Zfp35*-deficient* (Zfp35$^{-/-}$) *mice*

We found that moderate numbers of CD4 and CD8 T cells were present in Zfp35-deficient mice of a BALB/c and C57BL/6 back ground (Fig. 1*D* and data not shown). The cell surface expression of TCR-β, CD3ε, CD25, CD69, CD44, and CD62L on thymic and splenic CD4 and CD8 T cells was found to be comparable to those of controls (data not shown). In addition, anti-TCR-β mAb-, IL-2-, or peptide-induced proliferative responses were indistinguishable between wild-type and *Zfp35*$^{-/-}$ splenic CD4 T cells (data not shown). Thus, no obvious defect in the phenotype or the activation of *Zfp35*$^{-/-}$ splenic CD4 T cells was noted.

Downloaded from www.jimmunol.org on February 23, 2010

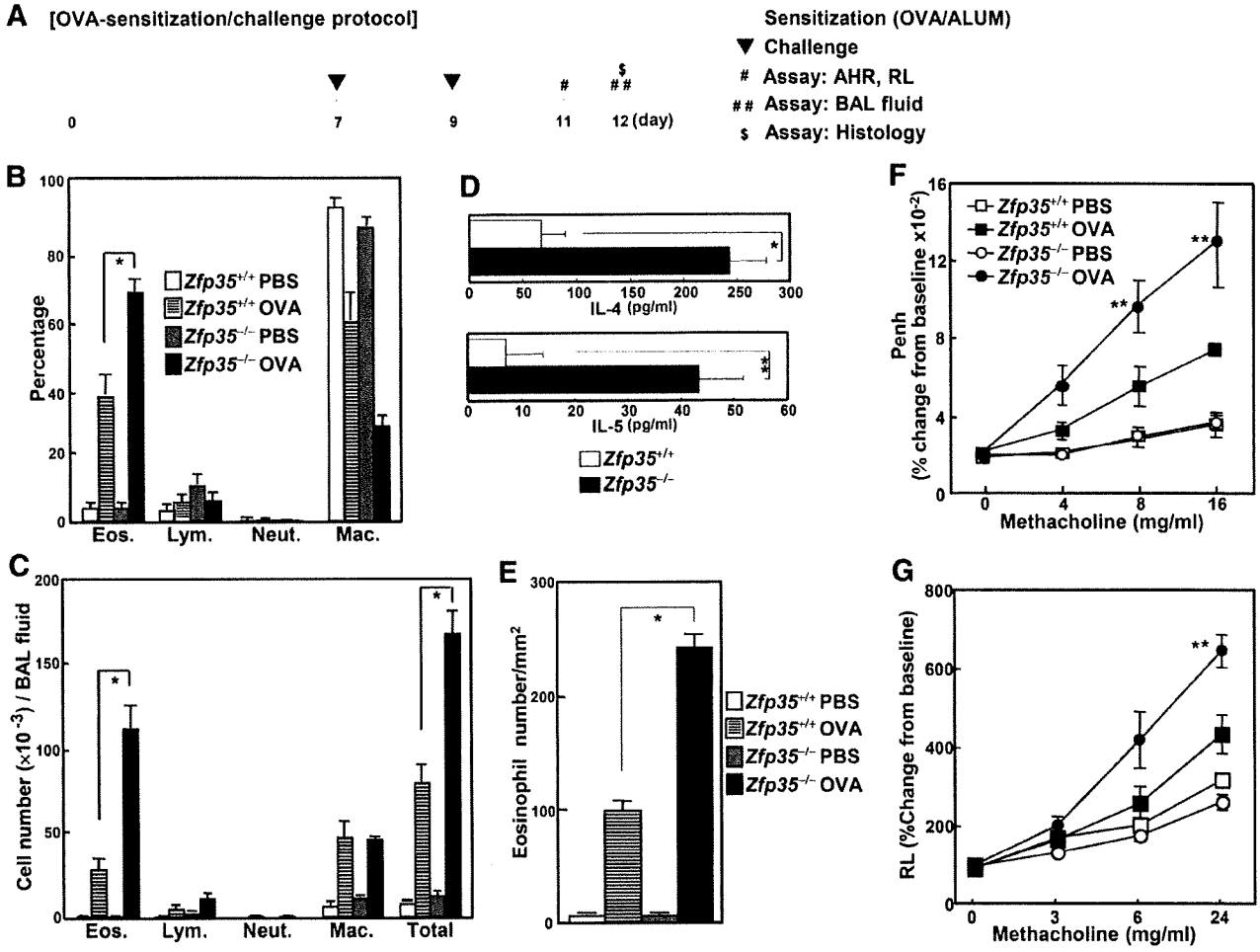

FIGURE 3. Increased OVA-induced airway inflammation and AHR in *Zfp35*$^{-/-}$ mice. *A*, BALB/c mice were injected i.p. with 250 μg of OVA in 4 mg of aluminum hydroxide gel on day 0. Mice were then treated intranasally with 100 μg of OVA in 30 μl of saline under anesthesia as described (challenge). On day 11, AHR and RL were assessed. On day 12, BAL fluid cells were prepared. Samples for histological analysis were prepared on day 12. The percentage (*B*) and absolute cell number (*C*) of eosinophils (Eos.), lymphocytes (Lym.), neutrophils (Neut.), and macrophages (Mac.) in BAL fluid are shown with SE. Four mice group were used. *, $p < 0.01$. *D*, Six hours after the second intranasal challenge, cytokine concentrations in the BAL fluid were measured by ELISA. The values with SDs are shown. Three mice per group were used. *, $p < 0.01$ and **, $p < 0.05$. *E*, The lungs were fixed and stained with Luna. The eosinophil numbers in the peribronchiolar region (mean cell number per mm^2 with SDs) are also shown. Three mice per group were used. *, $p < 0.01$. AHR in response to increasing doses of methacholine was assessed by measuring enhanced pause (Penh; *F*) or airway resistance (RL; *G*). Mean values of the percent above baseline are shown with SD. A total of three independent experiments was performed with similar results. *, $p < 0.01$ and **, $p < 0.05$.

Enhanced OVA- and anti-TCR Ab-induced Th2 cell differentiation in Zfp35$^{-/-}$ *mice*

To examine the influence of Th cell differentiation in the naive *Zfp35*$^{-/-}$ CD4 T cells, we used the in vitro Th1/Th2 cell differentiation method and examined the response by intracellular cytokine staining (40, 53). Naive splenic CD4 T cells (CD4$^+$ CD44^{low}) were purified by cell sorting (purity >98%). An assessment of the capability of *Zfp35*$^{-/-}$ CD4 T cells to differentiate into Th1/Th2 cells in vitro indicated a moderate enhancement of Th2 cell differentiation under Th2 conditions (18.8% vs 26.5% and 29.3% vs 42.3%; Fig. 2*B*), while Th1 cell differentiation was equivalent at the same IL-12 dose (Fig. 2*A*). The ability to produce Th2 cytokines was then assessed by ELISA. As shown in Fig. 2*E*, the production of IL-4, IL-5, and IL-13 increased about 2- to 4-fold in zfp35-deficient Th2 cells. IFN-γ production was not detectable in the cultured Th2 cells.

Next, to further examine the efficiency in Th2 cell differentiation of *Zfp35*$^{-/-}$ T cells, purified splenic CD4 T cells were stimulated with immobilized anti-TCRβ mAb in graded doses of exogenous cytokines. Th2 cell differentiation was enhanced in *Zfp35*$^{-/-}$ T cells at any doses of exogenous IL-4, particularly the enhancement was more prominent under relatively lower IL-4 conditions, whereas Th1 cell differentiation was unaffected (Fig. 2, *C* and *D*). In addition, proliferative responses induced with antigenic peptide, IL-2, or IL-4 were indistinguishable between wild-type and *Zfp35*$^{-/-}$ effector Th2 cells (data not shown). These results thus far suggest that Zfp35 regulates Th2 cell differentiation in a negative manner.

Enhanced OVA-induced eosinophilic inflammation and AHR in Zfp35$^{-/-}$ *mice*

To assess the role of Zfp35 in allergic airway inflammation, the BAL fluid of OVA-immunized and OVA-inhaled wild-type and *Zfp35*$^{-/-}$ (BALB/c background) mice was collected 48 h after the last OVA challenge (Fig. 3*A*). The number of total infiltrating cells and the absolute number of eosinophils and the percentages of eosinophils per

Downloaded from www.jimmunol.org on February 23, 2010

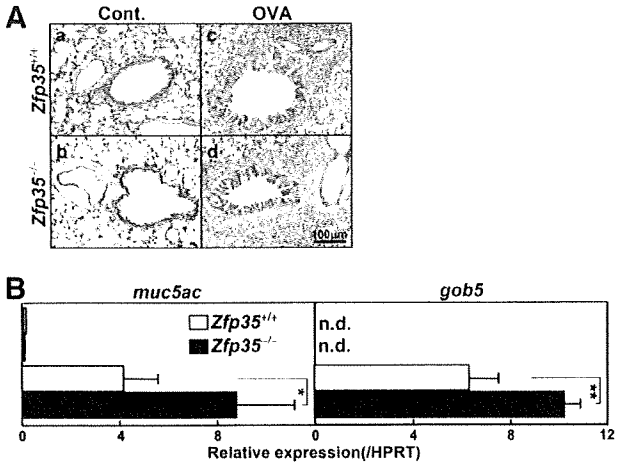

FIGURE 4. Hypermucus production in $Zfp35^{-/-}$ mice. *A*, Ag-induced goblet cell hyperplasia was evaluated by periodic acid-Schiff staining. Representative photographic views of wild-type and $Zfp35^{-/-}$ mice (BALB/c background) are shown (*a–d*). *B*, Total RNA was prepared from the lung of asthmatic wild-type or $Zfp35^{-/-}$ mice and mRNA levels of *muc5ac* and *gob5* were examined. The data represent the mean values of *muc5ac* and *gob5* mRNA expression normalized with *hprt* expression. Three independent experiments were done with similar results (*, $p < 0.01$ and **, $p < 0.05$). n.d., Not detected; Cont., control.

mouse increased significantly in $Zfp35^{-/-}$ mice (Fig. 3, *B* and *C*). The cytokines (IL-4, IL-5, IL-13, and IFN-γ) in the BAL fluid were also measured by ELISA. Under our conditions, IL-4 and IL-5 were detectable and were significantly increased in the $Zfp35^{-/-}$ mice (Fig. 3*D*). IL-13 and IFN-γ were undetectable in the BAL fluid. We evaluated the numbers of infiltrated eosinophils by Luna staining (Fig. 3*E*). The eosinophilic infiltration was observed to be enhanced in $Zfp35^{-/-}$ mice and the infiltration extended to the surrounding regions in $Zfp35^{-/-}$ mice (data not shown).

To evaluate the levels of AHR, OVA-immunized wild-type and $Zfp35^{-/-}$ mice were exposed to intranasal-treated OVA. Then AHR was assessed by measuring the methacholine-induced airflow obstruction in a whole-body plethysmograph and the respiratory system resistance using a computer-controlled small animal ventilator. As shown in Fig. 3, *F* and *G*, the augmented hyperresponsiveness to methacholine was detected in $Zfp35^{-/-}$ mice compared with $Zfp35^{+/+}$ control mice.

Specific staining of mucus-containing epithelial cells was not detected in wild-type or $Zfp35^{-/-}$ mice when OVA was not challenged (Fig. 4*A*, control (Cont.), *a* and *b*). After the OVA challenge, $Zfp35^{-/-}$ mice showed a mildly increased mucus production in the airway epithelium in comparison to wild-type mice (Fig. 4*A*, *c* and *d*). Subsequently, we examined the expression of *muc5ac* and *gob5* in the asthmatic lung of $Zfp35^{-/-}$ mice. The expression of these genes in the lung of $Zfp35^{-/-}$ mice significantly increased as compared wild-type mice (Fig. 4*B*). Taken together, these results indicated that allergic airway inflammation, mucus production, and AHR were all enhanced in $Zfp35^{-/-}$ mice. Thus, Zfp35 appears to be one of the key transcription factors in mediating Th2-dependent airway inflammation.

Increased Th2 cytokine production from CD4 T cells of BAL fluid in immunized Zfp35$^{-/-}$ *mice*

Th2 cells predominantly express CCR3 and CCR4 (54–56). Consequently, we examined the cell surface expression of CCR3 and CCR4 on CD4 T cells in OVA-immunized and -challenged $Zfp35^{-/-}$ mice. The expression of these chemokine receptors was very low either on $CD44^{high}$ or $CD44^{low}$ splenic CD4 T cells, and no difference was detected between wild-type and $Zfp35^{-/-}$ mice (Fig. 5*A*), thus indicating that CD4 T cells in the spleen of $Zfp35^{-/-}$ mice were not spontaneously polarized.

We also examined the expression of CD25, CD44, and CD69 on the splenic CD4 T cells and lung CD4 T cells in OVA-immunized and -challenged $Zfp35^{-/-}$ mice (Fig. 5*B*). The number of $CD25^+$ and $CD69^+$ CD4 T cells in the lung slightly increased in the

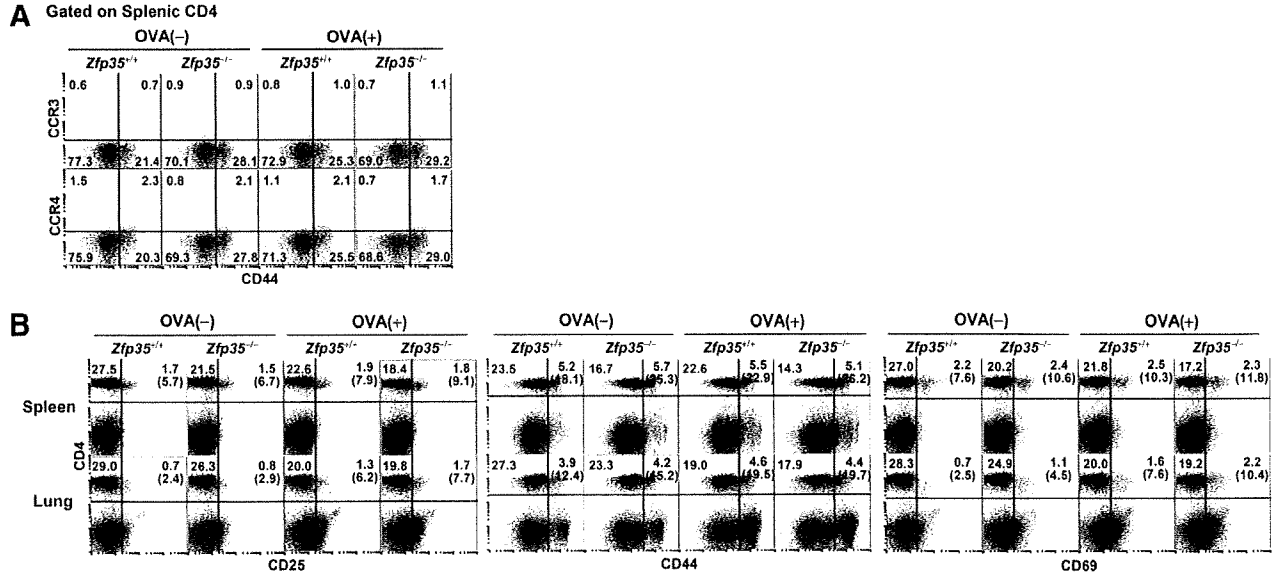

FIGURE 5. The expression of surface makers on CD4 T cells of OVA-immunized and -challenged $Zfp35^{-/-}$ mice. The mice were injected i.p. with OVA/alum on day 0. On days 7 and 9, the mice were treated intranasally with OVA (challenge). On day 12, lung mononuclear cells and splenocytes were prepared. *A*, Splenocytes were stained with anti-CD4, anti-CD44, and anti-CCR3 mAb or anti-CCR4 mAb. *B*, Splenocytes and lung mononuclear cells were stained with anti-CD4 and one of anti-CD25, anti-CD44, and anti-CD69 mAbs. The percentages of each quadrant are shown. The percentages among the CD4 T cells are given in parentheses. Three independent experiments were done with similar results.

Downloaded from www.jimmunol.org on February 23, 2010

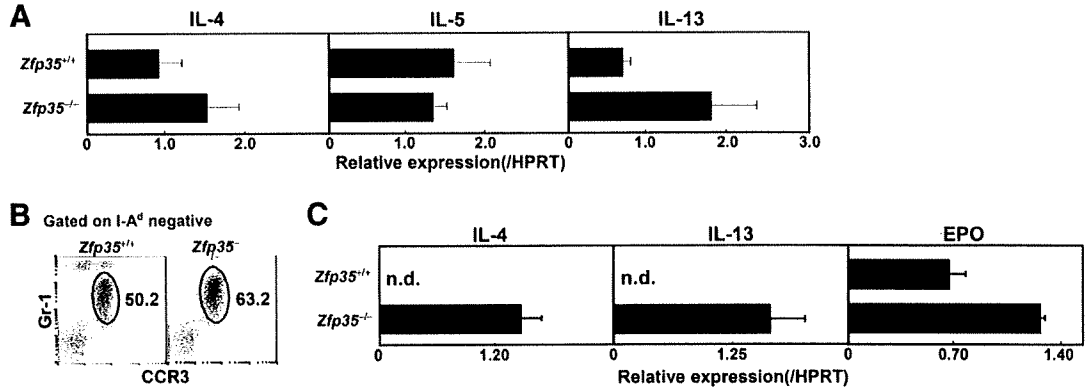

FIGURE 6. Increased Th2 cytokine production of CD4 T cells and eosinophils in the BAL fluid of OVA-immunized and -challenged *Zfp35*$^{-/-}$ mice. The mice were immunized and challenged with OVA as described in Fig. 5. On day 12, BAL fluid cells were prepared and pooled from 10 mice per group. CD4 T cells and I-A^d-negative, Gr-1, and CCR3-positive eosinophils were isolated by a cell sorter. *A*, The mRNA expression of IL-4, IL-5, and IL-13 in the BAL fluid CD4 T cells was assessed by quantitative RT-PCR. *B*, Eosinophils in the BAL fluid were stained with anti-I-A^d, anti-Gr-1, and anti-CCR3 mAbs. Representative staining profiles of CCR3/Gr-1 on I-A^d-negative cells are shown. Percentages of CCR3$^+$Gr-1$^+$ cells in the BAL fluid are also indicated. *C*, The mRNA expression levels of IL-4, IL-13, and EPO in the eosinophils are shown. n.d., Not detected. Three independent experiments were done with similar results.

OVA-immunized and -challenged mice in comparison to nonimmunized mice, but the numbers of CD25$^+$, CD44$^+$, and CD69$^+$ cells in the *Zfp35*$^{-/-}$ groups were comparable to those of the wild type. These results indicate that CD4 T cells in the spleen and the asthmatic lung of *Zfp35*$^{-/-}$ mice were not spontaneously activated even after OVA immunization and challenge.

Increased Th2 cytokine production from CD4 T cells and eosinophils in the BAL fluid in Zfp35$^{-/-}$ *mice*

We isolated the BAL fluid from OVA-immunized and -challenged *Zfp35*$^{-/-}$ mice, and CD4 T cells and I-A^d- negative, Gr-1, and CCR3-positive eosinophils were isolated by a cell sorter. The mRNA expression of IL-4, IL-5, and IL-13 in the BAL fluid CD4 T cells was assessed, and the expression of IL-4 and IL-13 was increased in *Zfp35*$^{-/-}$ mice (Fig. 6*A*). The percentages of I-A^d-negative, Gr-1, and CCR3- positive eosinophils were slightly increased (Fig. 6*B*). The levels of IL-4, IL-5, IL-13, and EPO mRNA expression in the sorted eosinophils were examined. The levels of IL-4, IL-13, and EPO expression were increased substantially in the *Zfp35*$^{-/-}$ groups in comparison to the wild type (Fig. 6*C*). The expression of IL-5 was not detected in this experimental system.

Modulation of airway inflammation by adoptively transferred Zfp35$^{-/-}$ *CD4 T cells*

Finally, we addressed whether OVA-primed T cells with altered Zfp35 expression are able to modulate OVA-induced allergic inflammation. Following immunization with OVA, splenic CD4 T cells from BALB/c and *Zfp35*$^{-/-}$ mice (BALB/c background) were prepared and transferred into BALB/c mice that had been also immunized with OVA once (Fig. 7*A*). Two and 4 days after cell transfer, mice were challenged with intranasal administration of OVA and the inflammatory infiltrates in the BAL fluid were analyzed. As shown in Fig. 7, *B* and *C*, the adoptive transfer of CD4 T cells from *Zfp35*$^{-/-}$ mice resulted in increased levels of eosinophilic infiltrates. As shown in Fig. 7, *D* and *E*, the hyperresponsiveness to methacholine in *Zfp35*$^{-/-}$ mice was enhanced compared with that in control mice. These results indicate that the expression levels of *Zfp35* in CD4 T cells appear to affect the OVA-induced airway inflammation and AHR.

Discussion

In this report, we demonstrated that *Zfp35*$^{-/-}$ CD4 T cells differentiate into Th2 cells more efficiently (Fig. 2). The development of eosinophilic airway inflammation, mucus hyperproduction, and AHR was shown to be enhanced in *Zfp35*$^{-/-}$ mice (Figs. 3 and 4). Th2 cytokine expression of CD4 T cells and eosinophils of BAL fluid in the challenged *Zfp35*$^{-/-}$ mice increased (Fig. 6). Moreover, the cell transfer of OVA-sensitized *Zfp35*$^{-/-}$ CD4 T cells modulated the airway inflammation (Fig. 7), thus indicating that Zfp35 plays an important role in the pathogenesis of airway inflammation and hyperresponsiveness through the control of Th2 cell generation and Th2 cytokine expression.

The absolute number of eosinophils in the BAL fluid is enhanced after OVA challenge (Figs. 3*C* and 7*C*). An increase in the percentage of eosinophils in the *Zfp35*$^{-/-}$ mice was also observed in the experiments shown in Fig. 3, and no remarkable change was observed in the cell transfer experiments (Fig. 7*B*). In addition, an increased IL-4 and IL-13 production in the eosinophils in the BAL fluid was detected (Fig. 6*C*). Thus, Zfp35 in Th2 cells and also in eosinophils appears to play an important role in the regulation of OVA-induced allergic airway inflammation.

No preferential expression of Zfp35 was detected between Th1 and Th2 cells (M. Kitajima and T. Nakayama, unpublished observation), while the enhancement of Th2 cell differentiation but not Th1 or Th17 cell differentiation was detected (Fig. 2 and our unpublished observation). GATA3 is one of crucial factors in Th2 differentiation and airway inflammation (57–59). Therefore, Zfp35 may regulate Th2-specific processes, such as those involving GATA3. However, the GATA3-dependent promoter activity on IL-5 promoter was not affected by Zfp35 (M. Kitajima and T. Nakayama, unpublished observation). Thus, Zfp35 appears to control a process that is required for Th2 cell differentiation but not GATA3-mediated transcriptional processes. Increasing numbers of transcription factors implicated in the development of allergic airway inflammation are reported; STAT factors, NF-κB, NFAT, AP-1 family protein, and Th2 cell-related transcription factors including GATA3, JunB, and c-Maf (60). Zinc finger transcription factors including Schnurri-2 (41) and repressor of GATA (ROG) (61) control the allergic airway inflammation.

The *Zfp35* gene was clustered with *znf191* and *znf397* in mouse chromosome 18A12 (62, 63). ZNF191 has been identified in a T cell line, contains four C_2H_2 zinc finger domains, and *znf191*-deficient mice died at ~7.5 days after fertilization (64). ZNF397 possesses nine C_2H_2 zinc finger domains and is expressed in the spleen and thymus at low levels and acts as a transcriptional

Downloaded from www.jimmunol.org on February 23, 2010

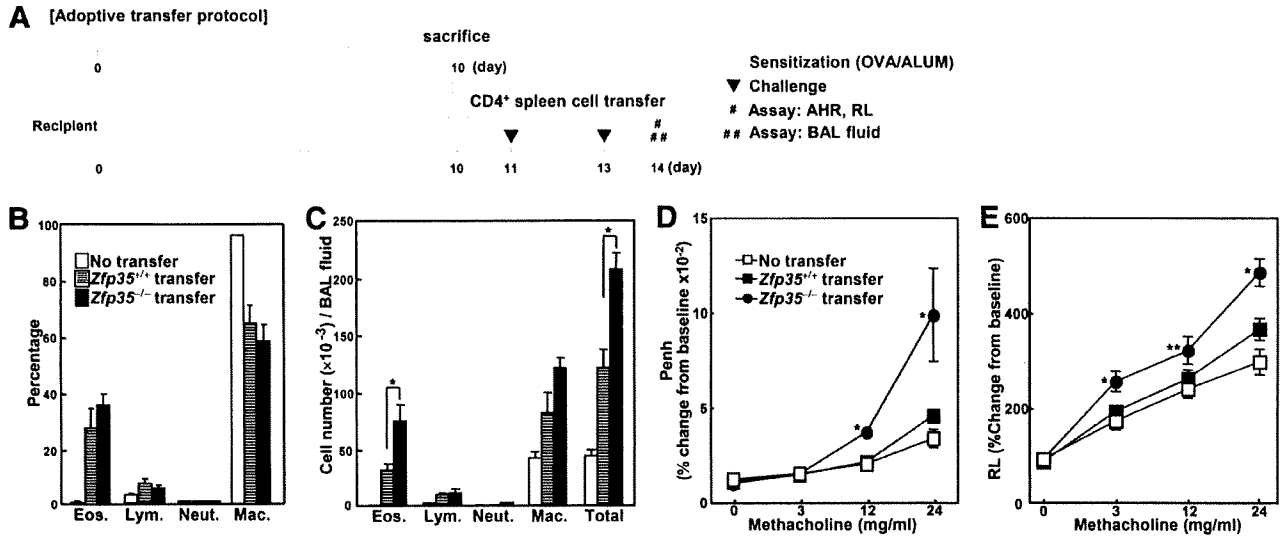

FIGURE 7. Increased airway inflammation and AHR induced by *Zfp35*$^{-/-}$ CD4 T cell transfer. *A*, Donor mice (*Zfp35*$^{+/+}$ or *Zfp35*$^{-/-}$ mice, BALB/c background) and recipient mice (BALB/c) were sensitized i.p. with 250 μg of OVA with alum on day 0. On day 10, splenic CD4 T cells were prepared from donor mice and transferred into recipient mice. The recipient mice were treated intranasally with 100 μg of OVA in 30 μl of saline under anesthesia on days 11 and 13. On day 14, AHR and RL were assessed. BAL fluid was collected on day 15. The percentage (*B*) and absolute cell number (*C*) of eosinophils (Eos.), lymphocytes (Lym.), neutrophils (Neut.) and macrophages (Mac.) in BAL fluid are shown. Four mice per group were used. AHR in response to increasing doses of methacholine was assessed by measuring enhanced pause (Penh; *D*) or airway resistance (RL; *E*). Mean values of the percentage above baseline are shown with SDs. A total of three independent experiments were performed with similar results. *, $p < 0.01$ and **, $p < 0.05$.

activator (63). The precise immunological function of these molecules was not investigated at this time. We examined the levels of mRNA expression of *znf191* and *znf397* in splenic *Zfp35*$^{-/-}$ CD4 T cells by a RT-PCR method, and the expression was found to be normal (M. Kitajima and T. Nakayama, unpublished observation). This indicates that the observed effects on Th2 cell differentiation and airway inflammation in Zfp35-deficient mice are not the result of an altered expression of the neighboring genes *znf191* and *znf397*in the same cluster.

The evolutional relationship among amino acid sequences of different Zfps with phylogenic tree analysis was reported (65). ZNF322 and ZNF328 are closely related to Zfp35 in the phylogenic tree (65, 66). ZNF322 contains nine zinc finger domains and regulates in a positive manner in MAPK signaling pathways. ZNF328 contains 15 zinc finger domains and 1 KRAB domain and regulates negatively the MAPK signaling pathways. Although no apparent effect of Zfp35 on the activation of the ERK MAPK cascades was detected in Th2 cells (M. Kitajima and T. Nakayama, unpublished observation), Zfp35 may also have a regulatory function on the MAPK signaling cascade in other cells.

ZNF^{EB} maps to human chromosome 18q12(62). The 18q12 region is known to be a hot spot for structural cytogenetic changes in numerous different malignancies (37). The mRNA expression of ZNF^{EB}, a human homolog of *Zfp35*, is transiently induced upon activation of human B cells by anti-IgM F(ab')$_2$ or a phorbol ester plus calcium ionophore (37). These observations suggest that ZNF^{EB} is a candidate key molecule involved in the pathogenesis of hematopoietic malignancies and immune disorders. Thus, Zfp35-deficient mice may provide a good experimental system for the analysis of the role of this interesting molecule.

Zinc deficiency was reported to be correlated with the Th2 inflammatory cytokine profile (67). Case-control studies in Scotland (68) and Spain (69) found that the combined risk of atopy, bronchial reactivity, and allergic-type symptoms were 4- to 5-fold higher in individuals with low zinc intake compared with those with higher zinc intakes. Significant decreases in serum, plasma, or hair zinc levels have also been reported in some asthmatic individuals (70). Intracellular Zn exists in two discreet pools, the first being nonexchangeable and tightly bound to metalloenzymes, and the second being a more labile and dynamic pool that is rapidly exchangeable and able to be altered by Zn deprivation or supplementation (71). It is possible that Zfp35 containing 18 continuous zinc (72) finger motifs partly maintain intracellular zinc homeostasis, thereby controlling allergic asthma.

Acknowledgments

We are grateful to Kaoru Sugaya, Toshihiro Ito, and Hikari Asou for excellent technical assistance.

Disclosures

The authors have no financial conflict of interest.

References

1. McFadden, E. R., Jr., and I. A. Gilbert. 1992. Asthma. *N. Engl. J. Med.* 327: 1928–1937.
2. Busse, W. W., and R. F. Lemanske, Jr. 2001. Asthma. *N. Engl. J. Med.* 344: 350–362.
3. Hamelmann, E., and E. W. Gelfand. 2001. IL-5-induced airway eosinophilia: the key to asthma? *Immunol. Rev.* 179: 182–191.
4. Lloyd, C. M., J. A. Gonzalo, A. J. Coyle, and J. C. Gutierrez-Ramos. 2001. Mouse models of allergic airway disease. *Adv. Immunol.* 77: 263–295.
5. Elias, J. A., C. G. Lee, T. Zheng, B. Ma, R. J. Homer, and Z. Zhu. 2003. New insights into the pathogenesis of asthma. *J. Clin. Invest.* 111: 291–297.
6. Kamata, T., M. Yamashita, M. Kimura, K. Murata, M. Inami, C. Shimizu, K. Sugaya, C. R. Wang, M. Taniguchi, and T. Nakayama. 2003. *src* homology 2 domain-containing tyrosine phosphatase SHP-1 controls the development of allergic airway inflammation. *J. Clin. Invest.* 111: 109–119.
7. Wills-Karp, M. 2004. Interleukin-13 in asthma pathogenesis. *Immunol. Rev.* 202: 175–190.
8. Cohn, L., J. A. Elias, and G. L. Chupp. 2004. Asthma: mechanisms of disease persistence and progression. *Annu. Rev. Immunol.* 22: 789–815.
9. Umetsu, D. T., and R. H. DeKruyff. 2006. The regulation of allergy and asthma. *Immunol. Rev.* 212: 238–255.

Downloaded from www.jimmunol.org on February 23, 2010

10. Infante-Duarte, C., H. F. Horton, M. C. Byrne, and T. Kamradt. 2000. Microbial lipopeptides induce the production of IL-17 in Th cells. *J. Immunol.* 165: 6107–6115.
11. Harrington, L. E., R. D. Hatton, P. R. Mangan, H. Turner, T. L. Murphy, K. M. Murphy, and C. T. Weaver. 2005. Interleukin 17-producing $CD4^+$ effector T cells develop via a lineage distinct from the T helper type 1 and 2 lineages. *Nat Immunol.* 6: 1123–1132.
12. Park, H., Z. Li, X. O. Yang, S. H. Chang, R. Nurieva, Y. H. Wang, Y. Wang, L. Hood, Z. Zhu, Q. Tian, and C. Dong. 2005. A distinct lineage of CD4 T cells regulates tissue inflammation by producing interleukin 17. *Nat Immunol.* 6: 1133–1141.
13. Bettelli, E., M. Oukka, and V. K. Kuchroo. 2007. T_H-17 cells in the circle of immunity and autoimmunity. *Nat. Immunol.* 8: 345–350.
14. Zhang, D. H., L. Cohn, P. Ray, K. Bottomly, and A. Ray. 1997. Transcription factor GATA-3 is differentially expressed in murine Th1 and Th2 cells and controls Th2-specific expression of the interleukin-5 gene. *J. Biol. Chem.* 272: 21597–21603.
15. Zheng, W., and R. A. Flavell. 1997. The transcription factor GATA-3 is necessary and sufficient for Th2 cytokine gene expression in CD4 T cells. *Cell* 89: 587–596.
16. Szabo, S. J., B. M. Sullivan, C. Stemmann, A. R. Satoskar, B. P. Sleckman, and L. H. Glimcher. 2002. Distinct effects of T-bet in T_H1 lineage commitment and IFN-γ production in CD4 and CD8 T cells. *Science* 295: 338–342.
17. Ivanov, I. I., B. S. McKenzie, L. Zhou, C. E. Tadokoro, A. Lepelley, J. J. Lafaille, D. J. Cua, and D. R. Littman. 2006. The orphan nuclear receptor RORγt directs the differentiation program of proinflammatory IL-17^+ T helper cells. *Cell* 126: 1121–1133.
18. Maldonado, E., M. Hampsey, and D. Reinberg. 1999. Repression: targeting the heart of the matter. *Cell* 99: 455–458.
19. Zawel, L., and D. Reinberg. 1995. Common themes in assembly and function of eukaryotic transcription complexes. *Annu. Rev. Biochem.* 64: 533–561.
20. Ghaleb, A. M., M. O. Nandan, S. Chanchevalap, W. B. Dalton, I. M. Hisamuddin, and V. W. Yang. 2005. Kruppel-like factors 4 and 5: the yin and yang regulators of cellular proliferation. *Cell Res.* 15: 92–96.
21. Venter, J. C., M. D. Adams, E. W. Myers, P. W. Li, R. J. Mural, G. G. Sutton, H. O. Smith, M. Yandell, C. A. Evans, R. A. Holt, et al. 2001. The sequence of the human genome. *Science* 291: 1304–1351.
22. Lander, E. S., L. M. Linton, B. Birren, C. Nusbaum, M. C. Zody, J. Baldwin, K. Devon, K. Dewar, M. Doyle, W. FitzHugh, et al. 2001. Initial sequencing and analysis of the human genome. *Nature* 409: 860–921.
23. Tupler, R., G. Perini, and M. R. Green. 2001. Expressing the human genome. *Nature* 409: 832–833.
24. Klug, A., and J. W. Schwabe. 1995. Protein motifs 5. Zinc fingers. *FASEB J.* 9: 597–604.
25. Bellefroid, E. J., P. J. Lecocq, A. Benhida, D. A. Poncelet, A. Belayew, and J. A. Martial. 1989. The human genome contains hundreds of genes coding for finger proteins of the Kruppel type. *DNA* 8: 377–387.
26. Safford, M., S. Collins, M. A. Lutz, A. Allen, C. T. Huang, J. Kowalski, A. Blackford, M. R. Horton, C. Drake, R. H. Schwartz, and J. D. Powell. 2005. Egr-2 and Egr-3 are negative regulators of T cell activation. *Nat. Immunol.* 6: 472–480.
27. Zhang, F., L. R. Thomas, E. M. Oltz, and T. M. Aune. 2006. Control of thymocyte development and recombination-activating gene expression by the zinc finger protein Zfp608. *Nat. Immunol.* 7: 1309–1316.
28. Kappes, D. J., X. He, and X. He. 2006. Role of the transcription factor Th-POK in CD4:CD8 lineage commitment. *Immunol. Rev.* 209: 237–252.
29. Zhu, J., D. Jankovic, A. Grinberg, L. Guo, and W. E. Paul. 2006. Gfi-1 plays an important role in IL-2-mediated Th2 cell expansion. *Proc. Natl. Acad. Sci. USA* 103: 18214–18219.
30. Kimura, M. Y., H. Hosokawa, M. Yamashita, A. Hasegawa, C. Iwamura, H. Watarai, M. Taniguchi, T. Takagi, S. Ishii, and T. Nakayama. 2005. Regulation of T helper type 2 cell differentiation by murine Schnurri-2. *J. Exp. Med.* 201: 397–408.
31. Kimura, M. Y., C. Iwamura, A. Suzuki, T. Miki, A. Hasegawa, K. Sugaya, M. Yamashita, S. Ishii, and T. Nakayama. 2007. Schnurri-2 controls memory Th1 and th2 cell numbers in vivo. *J. Immunol.* 178: 4926–4936.
32. Blanchard, A. D., K. R. Page, H. Watkin, P. Hayward, T. Wong, M. Bartholomew, D. J. Quint, M. Daly, J. Garcia-Lopez, and B. R. Champion. 2000. Identification and characterization of SKAT-2, a novel Th2-specific zinc finger gene. *Eur. J. Immunol.* 30: 3100–3110.
33. Kovalovsky, D., O. U. Uche, S. Eladad, R. M. Hobbs, W. Yi, E. Alonzo, K. Chua, M. Eidson, H. J. Kim, J. S. Im, P. P. Pandolfi, and D. B. Sant'Angelo. 2008. The BTB-zinc finger transcriptional regulator PLZF controls the development of invariant natural killer T cell effector functions. *Nat. Immunol.* 9: 1055–1064.
34. Sabater, L., Y. Ashhab, P. Caro, E. C. Kolkowski, R. Pujol-Borrell, and O. Dominguez. 2002. Identification of a KRAB-containing zinc finger protein, ZNF304, by AU-motif-directed display method and initial characterization in lymphocyte activation. *Biochem. Biophys. Res. Commun.* 293: 1066–1072.
35. Yasui, D. H., T. Genetta, T. Kadesch, T. M. Williams, S. L. Swain, L. V. Tsui, and B. T. Huber. 1998. Transcriptional repression of the IL-2 gene in Th cells by ZEB. *J. Immunol.* 160: 4433–4440.
36. Cunliffe, V., P. Koopman, A. McLaren, and J. Trowsdale. 1990. A mouse zinc finger gene which is transiently expressed during spermatogenesis. *EMBO J.* 9: 197–205.
37. Tune, C. E., M. Pilon, Y. Saiki, and H. M. Dosch. 2002. Sustained expression of the novel EBV-induced zinc finger gene, ZNFEB, is critical for the transition of B lymphocyte activation to oncogenic growth transformation. *J. Immunol.* 168: 680–688.
38. Strausberg, R. L., E. A. Feingold, L. H. Grouse, J. G. Derge, R. D. Klausner, F. S. Collins, L. Wagner, C. M. Shenmen, G. D. Schuler, S. F. Altschul, et al. 2002. Generation and initial analysis of more than 15,000 full-length human and mouse cDNA sequences. *Proc. Natl. Acad. Sci. USA* 99: 16899–16903.
39. Murphy, K. M., A. B. Heimberger, and D. Y. Loh. 1990. Induction by antigen of intrathymic apoptosis of $CD4^+CD8^+TCR^{low}$ thymocytes in vivo. *Science* 250: 1720–1723.
40. Yamashita, M., M. Kimura, M. Kubo, C. Shimizu, T. Tada, R. M. Perlmutter, and T. Nakayama. 1999. T cell antigen receptor-mediated activation of the Ras/mitogen-activated protein kinase pathway controls interleukin 4 receptor function and type-2 helper T cell differentiation. *Proc. Natl. Acad. Sci. USA* 96: 1024–1029.
41. Iwamura, C., M. Y. Kimura, K. Shinoda, Y. Endo, A. Hasegawa, M. Yamashita, and T. Nakayama. 2007. Schnurri-2 regulates Th2-dependent airway inflammation and airway hyperresponsiveness. *Int. Immunol.* 19: 755–762.
42. Yamashita, M., M. Katsumata, M. Iwashima, M. Kimura, C. Shimizu, T. Kamata, T. Shin, N. Seki, S. Suzuki, M. Taniguchi, and T. Nakayama. 2000. T cell receptor-induced calcineurin activation regulates T helper type 2 cell development by modifying the interleukin 4 receptor signaling complex. *J. Exp. Med.* 191: 1869–1879.
43. Kimura, M., Y. Koseki, M. Yamashita, N. Watanabe, C. Shimizu, T. Katsumoto, T. Kitamura, M. Taniguchi, H. Koseki, and T. Nakayama. 2001. Regulation of Th2 cell differentiation by mel-18, a mammalian polycomb group gene. *Immunity* 15: 275–287.
44. Nakayama, T., C. H. June, T. I. Munitz, M. Sheard, S. A. McCarthy, S. O. Sharrow, L. E. Samelson, and A. Singer. 1990. Inhibition of T cell receptor expression and function in immature $CD4^+CD8^+$ cells by CD4. *Science* 249: 1558–1561.
45. Yamashita, M., M. Kimura, M. Kubo, C. Shimizu, T. Tada, R. M. Perlmutter, and T. Nakayama. 1999. T cell antigen receptor-mediated activation of the Ras/mitogen-activated protein kinase pathway controls interleukin 4 receptor function and type-2 helper T cell differentiation. *Proc. Natl. Acad. Sci. USA* 96: 1024–1029.
46. Kimura, M. Y., H. Hosokawa, M. Yamashita, A. Hasegawa, C. Iwamura, H. Watarai, M. Taniguchi, T. Takagi, S. Ishii, and T. Nakayama. 2005. Regulation of T helper type 2 cell differentiation by murine Schnurri-2. *J. Exp. Med.* 201: 397–408.
47. Nigo, Y. I., M. Yamashita, K. Hirahara, R. Shinnakasu, M. Inami, M. Kimura, A. Hasegawa, Y. Kohno, and T. Nakayama. 2006. Regulation of allergic airway inflammation through Toll-like receptor 4-mediated modification of mast cell function. *Proc. Natl. Acad. Sci. USA* 103: 2286–2291.
48. Hansen, G., G. Berry, R. H. DeKruyff, and D. T. Umetsu. 1999. Allergen-specific Th1 cells fail to counterbalance Th2 cell-induced airway hyperreactivity but cause severe airway inflammation. *J. Clin. Invest.* 103: 175–183.
49. Foster, P. S., S. P. Hogan, A. J. Ramsay, K. I. Matthaei, and I. G. Young. 1996. Interleukin 5 deficiency abolishes eosinophilia, airways hyperreactivity, and lung damage in a mouse asthma model. *J. Exp. Med.* 183: 195–201.
50. Kamata, T., M. Yamashita, M. Kimura, K. Murata, M. Inami, C. Shimizu, K. Sugaya, C. R. Wang, M. Taniguchi, and T. Nakayama. 2003. src homology 2 domain-containing tyrosine phosphatase SHP-1 controls the development of allergic airway inflammation. *J. Clin. Invest.* 111: 109–119.
51. Takeda, K., E. Hamelmann, A. Joetham, L. D. Shultz, G. L. Larsen, C. G. Irvin, and E. W. Gelfand. 1997. Development of eosinophilic airway inflammation and airway hyperresponsiveness in mast cell-deficient mice. *J. Exp. Med.* 186: 449–454.
52. Koya, T., T. Kodama, K. Takeda, N. Miyahara, E. S. Yang, C. Taube, A. Joetham, J. W. Park, A. Dakhama, and E. W. Gelfand. 2006. Importance of myeloid dendritic cells in persistent airway disease after repeated allergen exposure. *Am. J. Respir. Crit. Care Med.* 173: 42–55.
53. Hosken, N. A., K. Shibuya, A. W. Heath, K. M. Murphy, and A. O'Garra. 1995. The effect of antigen dose on $CD4^+$ T helper cell phenotype development in a T cell receptor-α β-transgenic model. *J. Exp. Med.* 182: 1579–1584.
54. Bonecchi, R., G. Bianchi, P. P. Bordignon, D. D'Ambrosio, R. Lang, A. Borsatti, S. Sozzani, P. Allavena, P. A. Gray, A. Mantovani, and F. Sinigaglia. 1998. Differential expression of chemokine receptors and chemotactic responsiveness of type 1 T helper cells (Th1s) and Th2s. *J. Exp. Med.* 187: 129–134.
55. Sallusto, F., D. Lenig, C. R. Mackay, and A. Lanzavecchia. 1998. Flexible programs of chemokine receptor expression on human polarized T helper 1 and 2 lymphocytes. *J. Exp. Med.* 187: 875–883.
56. Sallusto, F., C. R. Mackay, and A. Lanzavecchia. 1997. Selective expression of the eotaxin receptor CCR3 by human T helper 2 cells. *Science* 277: 2005–2007.
57. Finotto, S., G. T. De Sanctis, H. A. Lehr, U. Herz, M. Buerke, M. Schipp, B. Bartsch, R. Atreya, E. Schmitt, P. R. Galle, et al. 2001. Treatment of allergic airway inflammation and hyperresponsiveness by antisense-induced local blockade of GATA-3 expression. *J. Exp. Med.* 193: 1247–1260.
58. Kiwamoto, T., Y. Ishii, Y. Morishima, K. Yoh, A. Maeda, K. Ishizaki, T. Iizuka, A. E. Hegab, Y. Matsuno, S. Homma, et al. 2006. Transcription factors T-bet and GATA-3 regulate development of airway remodeling. *Am. J. Respir. Crit. Care Med.* 174: 142–151.
59. Zhang, D. H., L. Yang, L. Cohn, L. Parkyn, R. Homer, P. Ray, and A. Ray. 1999. Inhibition of allergic inflammation in a murine model of asthma by expression of a dominant-negative mutant of GATA-3. *Immunity* 11: 473–482.
60. Yamashita, M., A. Onodera, and T. Nakayama. 2007. Immune mechanisms of allergic airway disease: regulation by transcription factors. *Crit. Rev. Immunol.* 27: 539–546.

Downloaded from www.jimmunol.org on February 23, 2010

61. Hirahara, K., M. Yamashita, C. Iwamura, K. Shinoda, A. Hasegawa, H. Yoshizawa, H. Koseki, F. Gejyo, and T. Nakayama. 2008. Repressor of GATA regulates T_H2-driven allergic airway inflammation and airway hyperresponsiveness. *J. Allergy Clin. Immunol.* 122: 512–520.
62. Huebner, K., T. Druck, C. M. Croce, and H. J. Thiesen. 1991. Twenty-seven nonoverlapping zinc finger cDNAs from human T cells map to nine different chromosomes with apparent clustering. *Am. J. Hum. Genet.* 48: 726–740.
63. Wu, Y., L. Yu, G. Bi, K. Luo, G. Zhou, and S. Zhao. 2003. Identification and characterization of two novel human SCAN domain-containing zinc finger genes ZNF396 and ZNF397. *Gene* 310: 193–201.
64. Li, J., X. Chen, H. Yang, S. Wang, B. Guo, L. Yu, Z. Wang, and J. Fu. 2006. The zinc finger transcription factor 191 is required for early embryonic development and cell proliferation. *Exp. Cell Res.* 312: 3990–3998.
65. Li, Y., Y. Wang, C. Zhang, W. Yuan, J. Wang, C. Zhu, L. Chen, W. Huang, W. Zeng, X. Wu, and M. Liu. 2004. ZNF322, a novel human C2H2 Kruppel-like zinc-finger protein, regulates transcriptional activation in MAPK signaling pathways. *Biochem. Biophys. Res. Commun.* 325: 1383–1392.
66. Ou, Y., S. Wang, Z. Cai, Y. Wang, C. Wang, Y. Li, F. Li, W. Yuan, B. Liu, X. Wu, and M. Liu. 2005. ZNF328, a novel human zinc-finger protein, suppresses transcriptional activities of SRE and AP-1. *Biochem. Biophys. Res. Commun.* 333: 1034–1044.
67. Prasad, A. S. 2000. Effects of zinc deficiency on Th1 and Th2 cytokine shifts. *J. Infect. Dis.* 182(Suppl. 1): S62–S68.
68. Soutar, A., A. Seaton, and K. Brown. 1997. Bronchial reactivity and dietary antioxidants. *Thorax* 52: 166–170.
69. de Luis, D. A., O. Izaola, R. Aller, A. Armentia, and L. Cuellar. 2003. [Antioxidant and fat intake in patients with polinic asthma]. *Med. Clin.* 121: 653–654.
70. Murgia, C., C. J. Lang, A. Q. Truong-Tran, D. Grosser, L. Jayaram, R. E. Ruffin, G. Perozzi, and P. D. Zalewski. 2006. Zinc and its specific transporters as potential targets in airway disease. *Curr. Drug Targets* 7: 607–627.
71. Truong-Tran, A. Q., R. E. Ruffin, and P. D. Zalewski. 2000. Visualization of labile zinc and its role in apoptosis of primary airway epithelial cells and cell lines. *Am. J. Physiol.* 279: L1172–L1183.
72. Maret, W., and B. L. Vallee. 1998. Thiolate ligands in metallothionein confer redox activity on zinc clusters. *Proc. Natl. Acad. Sci. USA* 95: 3478–3482.

Downloaded from www.jimmunol.org on February 23, 2010

The Runx3 Transcription Factor Augments Th1 and Down-Modulates Th2 Phenotypes by Interacting with and Attenuating GATA3[1]

Kazuyoshi Kohu,[2*‡] Hidetaka Ohmori,[2*] Won Fen Wong,[*] Daisuke Onda,[*] Takeshi Wakoh,[*] Shunsuke Kon,[*] Masakatsu Yamashita,[†] Toshinori Nakayama,[†] Masato Kubo,[‡] and Masanobu Satake[3*]

Recently, it was reported that the expression of Runt-related transcription factor 3 (Runx3) is up-regulated in CD4$^+$ helper T cells during Th1 cell differentiation, and that Runx3 functions in a positive feed-forward manner with the T-box family transcription factor, T-bet, which is a master regulator of Th1 cell differentiation. The relative expression levels of IFN-γ and IL-4 are also regulated by the Th2-associated transcription factor, GATA3. Here, we demonstrate that Runx3 was induced in Th2 as well as Th1 cells and that Runx3 interacted with GATA3 and attenuated GATA3 transcriptional activity. Ectopic expression of Runx3 in vitro in cultured cells or transgenic expression of Runx3 in mice accelerated CD4$^+$ cells to a Th1-biased population or down-modulated Th2 responses, in part by neutralizing GATA3. Our results suggest that the balance of Runx3 and GATA3 is one factor that influences the manifestation of CD4$^+$ cells as the Th1 or Th2 phenotypes. ***The Journal of Immunology,*** **2009, 183: 7817–7824.**

The CD4$^+$ helper T cells play a central role in acquired immunity. Naive CD4$^+$ T cells in peripheral lymphoid tissues are activated by Ag and induced to differentiate into effector Th cells, which secrete large amounts of effector cytokines. Distinct subsets of effector Th cells can be functionally defined by their discrete cytokine expression profiles. Th1 cells secrete IFN-γ, IL-2, and TNF-α and mediate defense against infection with intracellular microbes and isotype switching to IgG2a and IgG2b, whereas Th2 cells secrete IL-4, IL-5, and IL-13 and promote humoral response to extracellular pathogens and isotype switching to IgG1 and IgE (1). Differentiation of Th subsets is regulated and coordinated by a complex network of transcriptional regulators, including T-box family transcription factor (T-bet)[4] and GATA3 (2, 3). GATA3 is a master regulator of Th2 differentiation and activates Th2-specific cytokine genes primarily through epigenetic modification of the *IL-4* locus (4). Ectopic expression of GATA3 can induce Th2 cell differentiation even under conditions in which STAT6, a transducer of IL-4 signals, is absent, a situation that otherwise promotes Th1 cell differentiation (5). Furthermore, GATA3 is involved in the autoactivation of *GATA3* gene transcription (5). GATA3 is necessary for Th2-mediated immune responses in vivo, as demonstrated by the analysis of conditional *GATA3* knockout mice (6, 7). T-bet is a master regulator of Th1 cell differentiation, and activates Th1-specific cytokine genes while repressing Th2-related cellular programs (8). When naive CD4$^+$ T cells encounter Ag, *GATA3* is transiently transcribed during the early response phase, even under Th1 conditions. However, at the protein level, T-bet negatively regulates GATA3 activity through a physical interaction with GATA3, and it functions as an antagonist of Th2 differentiation (9).

The Runt-related transcription factors (Runx) harbor an evolutionarily conserved 128-aa region termed the Runt domain, which is responsible for DNA binding (10–12). Runx proteins interact with coactivators or corepressors to activate or repress target genes in a context-dependent manner (13). In thymocyte development, Runx1 and Runx3 are essential factors in the generation of CD8$^+$ cells. Runx1 and Runx3 have been shown to repress the expression of *CD4* and to activate the expression of *CD8* (14–16). Runx transcription factors are also involved in the regulation of Th cell differentiation. We previously reported that the forced expression of Runx1 in naive CD4$^+$ T cells promotes Th1 cell differentiation even under conditions that promote Th2 differentiation. Conversely, introduction of a dominant negative form of Runx1 biases cytokine secretion toward the Th2 phenotype (17). Recently, Djuretic et al. (18) demonstrated that Runx3 expression is up-regulated during Th1 differentiation and functions in a positive feed-forward manner in Th1 differentiation. They also demonstrated that in Th1 cells, Runx3 interacts with T-bet and simultaneously attenuates *IL-4* expression and augments *IFN-γ* expression. These effects are achieved by the binding of a Runx3/T-bet complex to the *IL-4* silencer and *IFN-γ* promoter, respectively. Thus, the interaction of Runx3 and T-bet appears to augment the activity of each binding partner, which explains why *Runx3*-deficient T cells are prone to Th2 differentiation.

*Institute of Development, Aging and Cancer, Graduate School of Life Sciences, Tohoku University, Sendai, Japan; †Department of Immunology, Graduate School of Medicine, Chiba University, Chiba, Japan; and ‡Laboratory for Signal Network, Research Center for Allergy and Immunology, The Institute of Physical and Chemical Research, Yokohama Institute, Yokohama, Japan

Received for publication August 1, 2008. Accepted for publication October 8, 2009.

The costs of publication of this article were defrayed in part by the payment of page charges. This article must therefore be hereby marked *advertisement* in accordance with 18 U.S.C. Section 1734 solely to indicate this fact.

[1] This work was supported in part by research grants from the Ministry of Education, Science, Sports, Culture and Technology, Japan. M.S. is a participant in the Global COE Program Network Medicine at Tohoku University.

[2] These authors contributed equally to this work.

[3] Address correspondence and reprint requests to Dr. Masanobu Satake, Institute of Development, Aging and Cancer, Tohoku University, Seiryo-machi 4-1, Aoba-ku, Sendai 980-8575, Japan. E-mail address: satake@idac.tohoku.ac.jp

[4] Abbreviations used in this paper: T-bet, T-box family transcription factor; HA, hemagglutinin; Runx, Runt-related transcription factor; ThN, Th cells under non-skewed conditions.

Copyright © 2009 by The American Association of Immunologists, Inc. 0022-1767/09/$2.00

www.jimmunol.org/cgi/doi/10.4049/jimmunol.0802527

Downloaded from www.jimmunol.org on February 23, 2010

The relative levels of IFN-γ and IL-4 expression are also regulated by the Th2-associated transcription factor GATA3. In this study, we present evidence that Runx3 associates with GATA3 and attenuates GATA3 transcriptional activity, thereby affecting cell phenotypes. The overexpression of Runx3 converted $CD4^+$ cells to a Th1-biased cell population and/or down-modulated Th2 responses, in part by neutralizing the activity of GATA3.

Materials and Methods

Cytokines and Abs

Mouse rIL-2, rIL-4, and rIL-12 were purchased from PeproTech. For T cell culture, anti-TCRβ (H57-597), anti-CD28 (37.51), anti-IL-4 (11B11), anti-IFN-γ (XMG1.2), and anti-IL-12 (C17.8) Abs were purchased from eBioscience. For intracellular cytokine staining, allophycocyanin-conjugated anti-IFN-γ (XMG1.2) and PE-conjugated anti-IL-4 (11B11) were purchased from BioLegend. The anti-Runx Ab was described previously (19). Anti-GATA3 (HG3-31), anti-α-tubulin (Ab-1), and anti-β-actin Abs were purchased from Santa Cruz Biotechnology and Calbiochem.

Cell culture and retrovirus infection

$CD4^+$ T cells were purified from the spleens of C57BL/6J (B6) mice using an IMag Cell Separation System (BD Biosciences). The purity of the $CD4^+$ fraction was >95% based on flow cytometry. Cells (2×10^5) were first stimulated with immobilized anti-TCRβ mAb (30 μg/ml) and soluble anti-CD28 mAb (10 μg/ml) in RPMI 1640 containing 10% (v/v) FBS for 2 days. To maintain cells under nonskewed (ThN) conditions, cells were cultured in the presence of IL-2 (30 U/ml) for an additional 7 days. For Th2 polarization, cells were cultured for 4 days in the presence of murine IL-4 (100 U/ml), anti-IL-12 Ab (10 μg/ml), and anti-IFN-γ Ab (10 μg/ml); for Th1 polarization, cells were cultured for 4 days in the presence of murine IL-12 (5 ng/ml) and anti-IL-4 Ab (10 μg/ml). Intracellular staining of IFN-γ and IL-4 was performed as described previously (17).

The murine *Runx3* cDNA was inserted into the retroviral expression vector pMX-GFP (17) to generate pMX-Runx3-IRES-GFP. Mutated versions of Runx3 were also inserted into pMX-GFP, and they were Runx3/1–404, Runx3/R178Q, and Runt each. Runx3/1–404 was constructed by PCR, whereas Runx3/R178Q (20) was provided by Drs. K. Ito and Y. Ito (National University of Singapore, Singapore). Runt represents a Runt domain derived from murine Runx1 (10). Both Runx3/R178Q and Runt function dominant negatively against intact Runx1/3 proteins. The *GATA3* cDNA was inserted into pMX-ratCD2 to generate pMX-GATA3-IRES-ratCD2. The packaging cell line PLAT-E was transfected with each plasmid using FugeneHD (Roche). After incubation for 24 h, the culture supernatant was harvested, concentrated, and used as a viral stock (21). $CD4^+$ T cells that had been stimulated as described for 24 h were infected with retroviruses using the DOTAP Liposomal Transfection Reagent (Roche) and then incubated under ThN-, Th1-, or Th2-permissive conditions for an additional 6 days. Rat $CD2^+$ cells were purified using a biotin-conjugated anti-rat CD2 Ab and an IMag Cell Separation System.

Immunoprecipitation and immunoblot analysis

293T cells were transfected with an expression vector, pcDNA3, encoding hemagglutinin (HA)-tagged Runx3 or GATA3 using the FugeneHD reagent (Roche). The Runt domain-deleted Runx3 and the Runt domain itself of Runx3 were also transfected into 293T cells. After incubation for 48 h, the cells were lysed in buffer containing 50 mM Tris-HCl (pH 7.4), 150 mM NaCl, 1% (v/v) Triton X-100, 1 mM $NaVO_4$, 1 mM NaF, and 1 μg/ml aprotinin. The lysates were also prepared from splenic $CD4^+$ T cells that had been cultured under Th2 conditions described previously. Each lysate was incubated with anti-HA (3F10; Roche) or anti-GATA3 (HG3-31) mAb, and the immunoprecipitates were adsorbed to protein G-Sepharose beads (GE Healthcare). The beads were washed five times with lysis buffer, and then proteins were eluted by boiling the beads in SDS sample buffer. As a control, whole-cell lysate was prepared by sonicating cells in SDS sample buffer. Proteins were resolved by SDS-PAGE and transferred to an Immobilon-P membrane (Millipore). The membrane was probed with an appropriate primary Ab, followed by an alkaline phosphatase-conjugated secondary Ab (Promega). Immune complexes were detected using NBT-5-bromo-4-chloro-3-indolyl phosphate reagents (Promega).

Semiquantitative RT-PCR analysis

RNA was isolated from cells using the ISOGEN reagent (Nippon Gene). First-strand cDNA was synthesized from RNA using Superscript II reverse transcriptase (Invitrogen Life Technologies). PCR amplification was performed under nonsaturating conditions using cDNA as the template and LA-*Taq* polymerase (Takara). The sequences of the sense and antisense primers were as follows: for *T-bet*, 5′-CTAAGCAAGGACGGCGAATGT-3′ and 5′-GGCTGGGAACAGGATACTGG-3′; for *IFN-γ*, 5′-GGTGACATGAAAATCCTGCAGAGC-3′and 5′-TCAGCAGCGACTCCTTTTCCGCTT-3′; for *TNF-α*, 5′-ATCAGTTCTATGGCCCAGACCCT-3′ and 5′-TCACAGAGCAATGACTCCAAAGTA-3′; for *IL-12*, 5′-GGGACATCATCAAACCAGACC-3′ and 5′-GCCAACCAAGCAGAAGACAGC-3′; for *IL-18*, 5′-ACTGTACAACCGCAGTAATAC-3′ and 5′-AGTGAACATTACAGATTTATCCC-3′; for *GATA3*, 5′-CTCCTTTTTGCTCTCCTTTTC-3′ and 5′-AAGAGATGAGGACTGGAGTG-3′; for *IL-4*, 5′-TCCACGGATGCGACAAAAAT-3′ and 5′-TTCTTCTTCAAGCATGGAGT-3′; for *IL-5*, 5′-GAGCACAGTGGTGAAAGAGACCTT-3′ and 5′-ATGACAGGTTTGGATAGCATTT-3′; for *IL-13*, 5′-AGTTCTACAGCTCCCTGGTTCTCT-3′ and 5′-CTTTGTGTAGCTGAGCAGTTTTGT-3′; for *Runx1*, 5′-ACTCTGCCGTCCATCTCCGACCCGC-3′ and 5′-CGTCGCTCTGGCTGGGGAGGCTGGG-3′; for *Runx3*, 5′-GCTGCAGAGCCTCACAGAGAGCCGC-3′ and 5′-GTCGGCTTCCACGCCATCAGGCTGG-3′; for *β-actin*, 5′-GATGACGATATCGCTGCGCTG-3′ and 5′-GTACGACCAGAGGCATACAGG-3′.

Luciferase reporter assay

M12 cells were cotransfected with a luciferase reporter plasmid and an expression plasmid for Runx3 or GATA3 using FugeneHD (Roche). As an internal control, cells were also transfected with pRL-TK (Promega), and the activity of *Renilla* luciferase was used to normalize for transfection efficiency. The cells were incubated for 24 h after transfection and then lysed in a passive lysis buffer (Promega). Luciferase activity was measured using a luciferase substrate (Promega) and a LumatLB9507 (Berthold Technologies).

EMSA

The procedure for the EMSA was described previously (15). The GATA binding sequence from the *IL-5* promoter, 5′-GGTGTCCTCTATCTGATTGTT-3′, was used as a probe to detect GATA DNA-binding activity. GATA3, Runx3, and CBFβ polypeptides were synthesized in vitro using the TnT T7 Coupled Reticulocyte Lysate System (Promega) and each cDNA template in a pcDNA3 vector.

Mice

The transgenic mouse line expressing a murine *Runx3* transgene was previously described (15). Litters of transgenic mice were backcrossed with B6 mice for 10 generations. B6 mice were purchased from Clea Japan. *Stat6*-deficient mice were obtained from Dr. S. Akira (Osaka University, Osaka, Japan) (22). Experiments were performed using 8- to 12-wk-old, age-matched mice. Mice were maintained and bred according to the guidelines defined by the Animal Facility of the Institute of Development, Aging and Cancer at Tohoku University (Sendai, Japan). All animal protocols used in this study were approved by our Institutional Animal Care and Use Committees.

Immunization, ELISA, and histology

Mice were injected s.c. with 10 μg of OVA (Sigma-Aldrich) in CFA or i.p. with 10 μg of OVA in aluminum hydroxide. Boosting injections were conducted at days 14 and 28. The titer of serum Ig was measured by ELISA. HRP-conjugated anti-mouse IgG1, anti-mouse IgG2a, anti-mouse IgG2b, and anti-mouse IgE were purchased from Bethyl. Spleens were isolated and fixed in 4% (w/v) paraformaldehyde in PBS for 18 h and then embedded in Tissue-Tek OCT compound (Sakura Finetechnical). Microsections of tissues on slides were stained by HRP-conjugated peanut agglutinin and counterstained with hematoxylin.

Results

Expression profiles of Runx proteins in nonskewed and differentiated Th cells

To examine the expression of Runx proteins during Th cell differentiation, naive $CD4^+$ cells were isolated from the spleens of mice and subjected to immunoblot analysis using an anti-pan-Runx Ab. The advantage of this Ab was that we could visualize the levels of each Runx family member simultaneously (the authenticity of Runx bands detected by the Ab had been confirmed previously in Refs. 15 and 19). As seen in Fig. 1, Runx1 was the sole major Runx component expressed in naive $CD4^+$ cells (Fig.

Downloaded from www.jimmunol.org on February 23, 2010

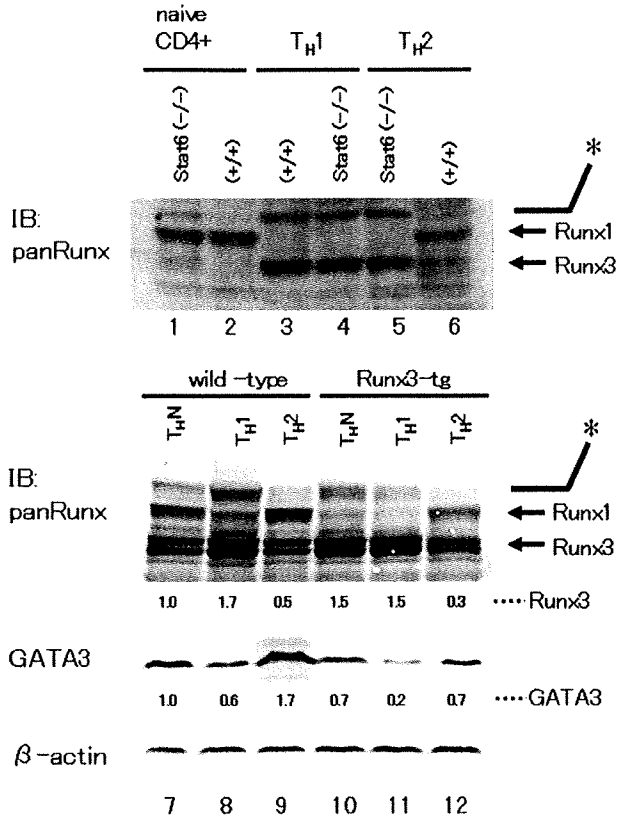

FIGURE 1. Expression of Runx proteins during Th cell differentiation. Immunoblot (IB) analysis of Runx proteins in naive $CD4^+$ cells and in $CD4^+$-derived Th cells cultured in vitro under ThN, Th1, or Th2 conditions for 7 days. $CD4^+$ T cells were isolated from the spleens of wild-type (+/+), *Stat6*-deficient (*Stat6*−/−) and *Runx3*-transgenic mice, as indicated. Extracts were probed with an anti-pan-Runx Ab. Arrows, Runx1 and Runx3. In the third panel from the top, extracts were also probed with an anti-GATA3 Ab. β-Actin served as a loading control. Relative densities of Runx3 and GATA3 bands are indicated below the gel. The identity of the protein indicated by the asterisk is unknown; however, based on its apparent m.w., it might represent Runx2.

1, *lane 2*). In contrast, in Th1-differentiated cells, Runx1 was undetectable, and Runx3 emerged as the principal Runx component (Fig. 1, *lane 3*). Th2-differentiated cells expressed equivalent amounts of Runx1 and Runx3 (Fig. 1, *lane 6*). In *Stat6*-deficient cells under Th2-promoting conditions, Runx expression was converted to a Th1-specific phenotype (Fig. 1, *lane 5*), which indicated that the expression of Runx proteins in wild-type Th2 cells is dependent on *Stat6*. When wild-type $CD4^+$ cells were stimulated through the TCR using an anti-TCRβ Ab and then cultured under nonskewed conditions, the expression patterns of Runx proteins were similar to those of Th2 cells (Fig. 1, compare *lanes 7* and *9*). These results indicated that Runx3 is not a Th1-specific factor but is expressed in TCR-stimulated $CD4^+$ cells as well as in Th2-differentiated cells.

Overexpression of Runx3 can activate IFN-γ and silence IL-4 expression even under conditions that promote Th2 differentiation

Previously, we reported that the expression of Runx1 in Th2 cells attenuates the exacerbation of the Th2 response (17). To determine whether Runx3 functioned in a similar manner, $CD4^+$ cells were cultured under conditions that promoted Th2 differentiation, and

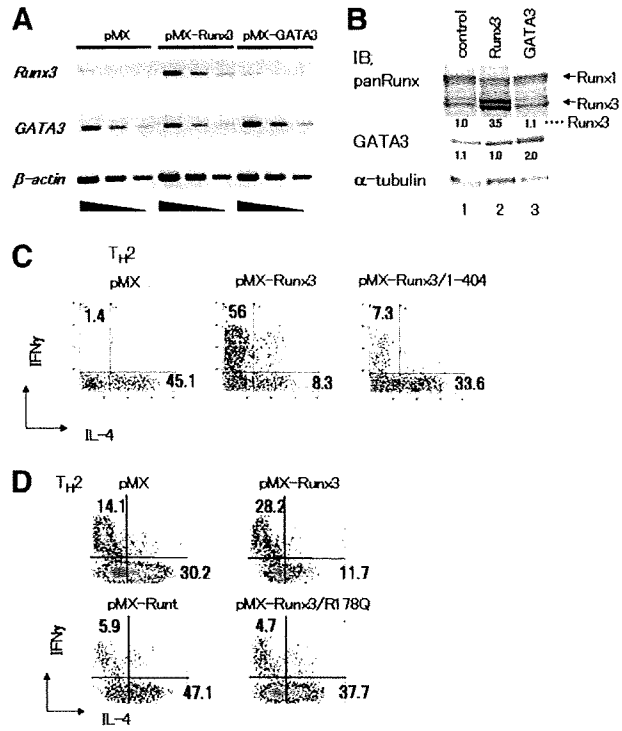

FIGURE 2. Effect of Runx3 expression on the expression of GATA3, and the relative levels of IFN-γ and IL-4. *A*, Semiquantitative RT-PCR analysis of *Runx3* and *GATA3* transcripts. Naive $CD4^+$ cells were isolated from the spleens of wild-type (WT) mice, stimulated with TCR, and then infected by a retrovirus carrying pMX-IRES-rCD2, pMX-Runx3-IRES-rCD2, or pMX-GATA3-IRES-rCD2, as indicated. After 7 days in culture under Th2 conditions, rat CD2-positive cells were isolated by cell sorting, and RNA was isolated and converted to cDNA. Increasing amounts of cDNA were used as the template for the detection of *Runx3* and *GATA3* transcripts by PCR. β-Actin was analyzed as a control. *B*, Immunoblot analysis of Runx1, Runx3, and GATA3 in Runx3- or GATA3-expressing cells. Lanes are as described for *A*, with the exception that α-tubulin was analyzed as a loading control. *C*, Naive $CD4^+$ cells were isolated from the spleens of wild-type mice, stimulated with TCR, and infected by a retrovirus carrying pMX-IRES-GFP, pMX-Runx3-IRES-GFP, or pMX-Runx3/1–404-IRES-GFP, as indicated. After 7 days in culture under Th2 conditions, the cells were restimulated and analyzed by intracellular staining for IFN-γ and IL-4, followed by flow cytometry. The fluorescence intensity of IFN-γ and IL-4 in the GFP-positive gated cell population is displayed. The numbers represent the percentage of cells in each quadrant. *D*, Effect of reducing endogenous Runx activity on IL-4 and IFN-γ expression. Experimental conditions were similar to those in *C*, except that cells were infected by a retrovirus carrying pMX-Runt-IRES-GFP and pMX-Runx3/R178Q-IRES-GFP and that the Th2 bias was far less prominent than in *C* (compare pMX-infected cells in *C* and *D*).

then infected by a retrovirus that was engineered to express *Runx3*. The overexpression of exogenous Runx3 in Th2 cells was confirmed by RT-PCR and immunoblot analysis (Fig. 2, *A* and *B*). The expression of Runx3 protein in infected cells was ~3.5-fold higher than in control Th2 cells (Fig. 2*B*, compare *lanes 1* and *2*). Fig. 1*C* shows the results of the analysis of intracellular IFN-γ and IL-4 levels in Th2 cells by flow cytometry. In control, pMX-infected cells, 45% of the cells were IL-4 positive, whereas only 1% were IFN-γ positive. In cells that overexpressed *Runx3*, this ratio was reversed, and 56% of the cells were IFN-γ positive whereas 8% were IL-4 positive. These results indicated that the overexpression of *Runx3* can activate IFN-γ expression and silence IL-4 expression, even under conditions that promote Th2 differentiation. The level of

Downloaded from www.jimmunol.org on February 23, 2010

GATA3 was not affected by the overexpression of Runx3 (Fig. 2*B*, compare *lanes 1* and 2). Thus, the observed effect of Runx3 on IFN-γ and IL-4 expression was not likely to be mediated through the modulation of GATA3 expression (however, the *T-bet* transcript was induced by the overexpressed Runx3; supplemental Fig. 1).[5]

The C-terminal five amino acid residues of Runx proteins comprise a characteristic VWRPY motif, with which a Groucho/TLE repressor interacts. To determine whether this motif contributed to Runx3-mediated *IL-4* repression, we expressed a mutant of Runx3 in which this motif was deleted (Runx3/1–404). As seen in Fig. 2*C*, 34% of cells that expressed Runx3/1–404 were IL-4 positive, whereas 7% were IFN-γ positive.

Reduction of endogenous Runx3 activity augments Th2 responses

Endogenous Runx3 activity was then artificially reduced to see its effect on IL-4 and IFN-γ expression. In Fig. 2*D*, $CD4^+$ cells were cultured under Th2 conditions but with less efficacy (the ratio of $IL\text{-}4^+$ to $IFN\text{-}\gamma^+$ cells in pMX of Fig. 2*D* was 2.1 as compared with 32 in pMX of Fig. 2*C*) and were infected by a retrovirus carrying pMX-Runt-IRES-GFP and pMX-Runx3/R178Q-IRES-GFP. The Runt domain and Runx3/R178Q are known to function dominant negatively against endogenous Runx protein, thereby reducing Runx activity inside the cells (10, 20). Ratios of $IL\text{-}4^+$ to $IFN\text{-}\gamma^+$ cells were 8.0 for both Runt- and Runx3/R178Q-infected cells. Compared with pMX-infected control cells, reduction of Runx activity resulted in a significant increase of $IL\text{-}4^+$ cells.

Runx3 interacts with GATA3 and attenuates GATA3 transcriptional activity

Runx1 has been shown to directly interact with GATA1 during megakaryocyte differentiation (23). As shown above, Runx3 was detected not only in Th1 but also in ThN and Th2 cells. To determine whether Runx3 interacted with GATA3, 293T cells were cotransfected with expression vectors for GATA3 and HA-tagged Runx3 and then subjected to immunoprecipitation using an anti-HA Ab, followed by immunoblot analysis using an anti-GATA3 Ab. As seen in Fig. 3, Runx3 and GATA3 coimmunoprecipitated with each other (Fig. 3*A*, *lane 4*). The Runt domain of Runx1 is critical for its association with GATA1 (23). When we transfected cells with a mutant of Runx3 in which the Runt domain was deleted, Runx3 and GATA3 failed to coimmunoprecipitate (Fig. 3*B*, *lane 9*). The Runx3 Runt domain alone, however, coimmunoprecipitated with GATA3 (Fig. 3*B*, *lane 10*).

Next, to determine whether endogenous GATA3 interacted with Runx3, cell lysates were prepared from $CD4^+$ T cells that were cultured under Th2 conditions and subjected to immunoprecipitation using anti-GATA3 Ab (Fig. 3*C*). Endogenous Runx3 coimmunoprecipitated together with endogenous GATA3 (see the band indicated by the arrowhead in Fig. 3*C*, *lane 13*). These results indicated that Runx3 interacts with GATA3.

To examine the functional significance of the Runx3-GATA3 interaction, we conducted a luciferase reporter gene assay in which luciferase expression was driven by the *IL-5* promoter. *IL-5* is a well-characterized GATA3-responsive Th2-specific gene in reporter gene assays (24). A fragment of the *IL-5* promoter spanning 1200 nt upstream of the transcription initiation site was ligated to the luciferase coding sequence (Fig. 4*A*). The promoter fragment contained 2 Runx sites (at positions −1030 and −470 relative to the transcriptional start site) and 1 GATA site (−20 nt). M12 B cells were cotransfected with the *IL-5*-luciferase reporter construct and expression vectors for Runx3 and/or GATA3. As indicated in Fig. 4*B*, the expression of GATA3 alone enhanced luciferase activity through the *IL-5* promoter 4-fold as compared with mock, whereas Runx3 had only a marginal effect. However, coexpression of Runx3 and GATA3 completely attenuated the enhancement of luciferase activity by GATA3. Mutation of the GATA site of the 1200-nt *IL-5* promoter fragment abolished its responsiveness to GATA3. A shorter fragment of the *IL-5* promoter (460 nt), which did not contain either of the Runx sites, was similar to the longer

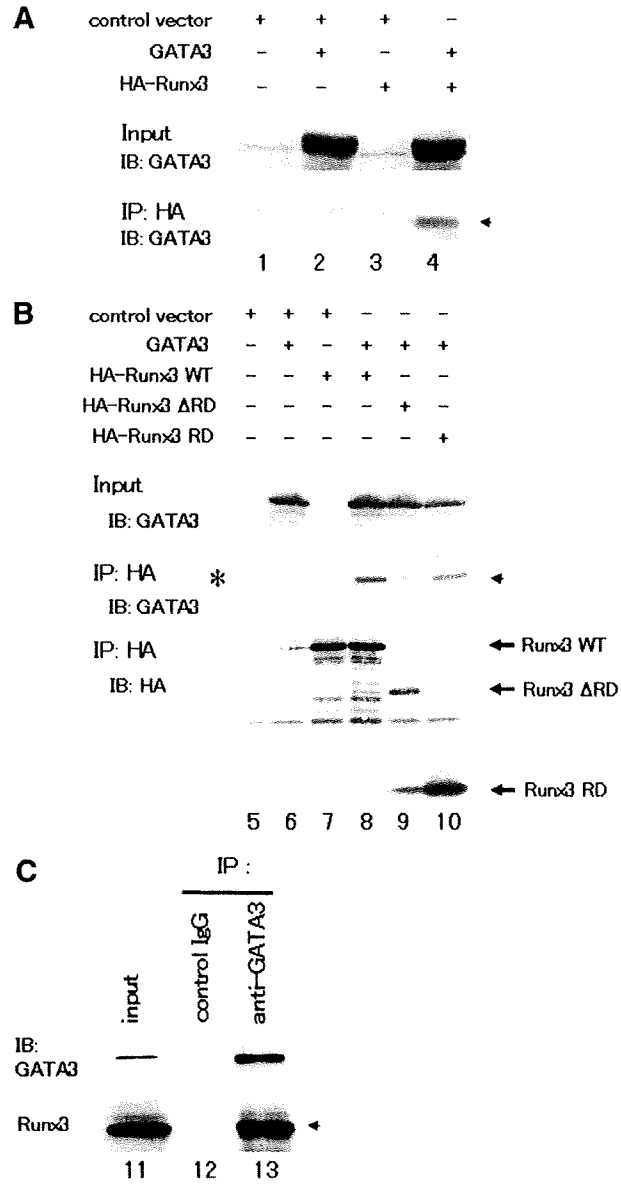

FIGURE 3. Physical interaction of Runx3 and GATA3. *A* and *B*, 293T cells were transfected with the indicated expression vectors for GATA3 and HA-tagged Runx3 or Runx3 mutants (Runt domain-deleted Runx3 or the Runx3 Runt domain alone). Lysates were prepared and subjected to immunoprecipitation (IP) using anti-HA Ab-conjugated protein G-Sepharose, followed by immunoblot (IB) analysis using an anti-GATA3 Ab. Arrowhead, GATA3. *C*, Interaction of endogenous GATA3 and Runx3 proteins. $CD4^+$ T cells were isolated from the spleen of wild-type mice, stimulated with TCR, and cultured under Th2 conditions for 7 days. The lysates were prepared and subjected to immunoprecipitation using anti-GATA3 mAb or control IgG. The precipitates were immunoblotted by anti-pan-Runx Ab. Arrowhead, Runx3.

[5] The online version of this article contains supplemental material.

Downloaded from www.jimmunol.org on February 23, 2010

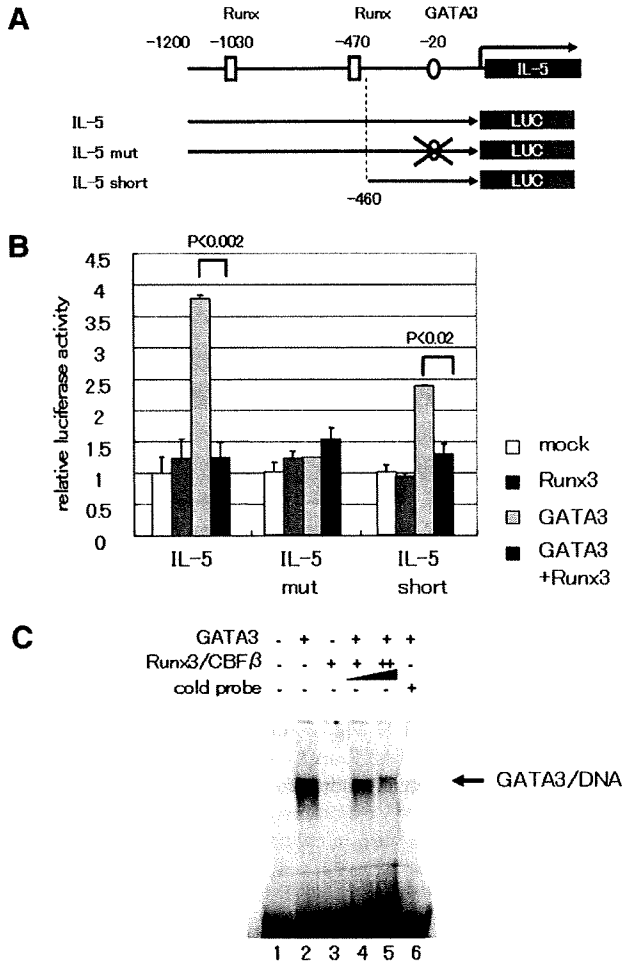

FIGURE 4. Effect of Runx3 and GATA3 on the activity of the *IL-5* promoter. *A*, Schematic illustration of the luciferase (LUC) reporter plasmid, in which luciferase expression is driven by the murine *IL-5* promoter. The 1200-nt region upstream of the transcriptional initiation site of *IL-5* harbors 2 Runx sites (at nt −1030 and −470 relative to the transcriptional start site) and 1 GATA site (at nt −20). This 1200-nt fragment was ligated to a luciferase reporter gene. The *IL-5* promoter in which the GATA site was mutated (mut), and a shorter 460-nt fragment of the *IL-5* promoter were also ligated to the luciferase reporter gene. *B*, M12 cells were transfected with the indicated luciferase reporter plasmid together with pcDNA3, pcDNA3-GATA3, and/or pcDNA3-Runx3. Data are the means ± SD of three independent experiments. Statistically significant differences were determined by the *t* test and are indicated by brackets (*p* values are indicated for each panel). *C*, EMSA of GATA3 and Runx3 proteins to the *IL-5* promoter sequence. GATA3, Runx3, and CBFβ proteins were synthesized from the respective cDNA in vitro, incubated with a radiolabeled oligonucleotide probe spanning the GATA-binding sequence of the *IL-5* promoter, and processed to EMSA. Proteins were added as in the indicated combinations, whereas a cold probe means an excessive amount of nonlabeled oligonucleotide.

1200-nt promoter fragment in its responsiveness to GATA3 and/or Runx3.

EMSA was then performed using a GATA binding sequence from the *IL-5* promoter as a probe (Fig. 4*C*). GATA3 and Runx3/CBFβ proteins were synthesized in vitro from the respective cDNAs and used. As expected, GATA3 but not Runx3 bound to the *IL-5* promoter (Fig. 4*C*, *lanes 2* and *3*). Coexistence of Runx3/CBFβ abolished DNA binding activity of GATA3 in a dose dependent manner (Fig. 4*C*, *lanes 4* and *5*). These results indicated

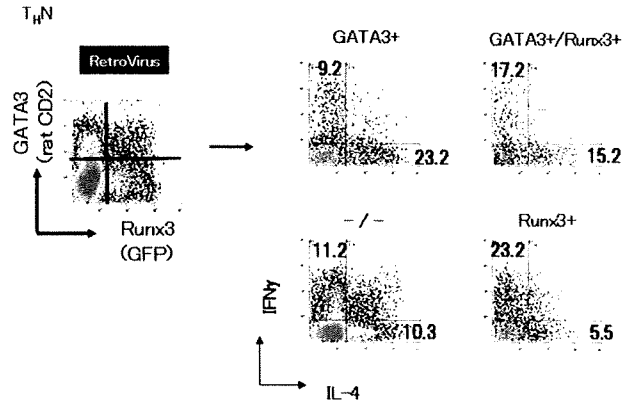

FIGURE 5. Effect of coexpression of Runx3 and GATA3 on IFN-γ and IL-4 expression. Naive $CD4^+$ cells were isolated from the spleens of wild-type mice, stimulated with TCR, and then doubly infected by retroviruses carrying pMX-Runx3-IRES-GFP and pMX-GATA3-IRES-ratCD2. After 7 days in culture under nonskewing conditions, the cells were restimulated and then analyzed by intracellular staining for IFN-γ and IL-4, followed by flow cytometry. The cells were gated into four subpopulations based on GFP- and rat CD2-specific fluorescence (*left*): GFP-negative/rat CD2-negative (*bottom left*); GFP-positive/rat CD2-negative (*bottom right*); GFP-negative/rat CD2-positive (*top left*); and GFP-positive/rat CD2-positive (*top right*). The fluorescence intensity of IFN-γ and IL-4 is shown for each subpopulation. Numbers represent the percentages of cells in each quadrant.

that Runx3 can interact with GATA3 and attenuate GATA3 transcriptional activity by inhibiting DNA-binding activity of GATA3. Thus, the mechanism of action of Runx3 and GATA3 is quite distinct from that of Runx3 and T-bet, in which the two factors interact with each other and augment the transcriptional activity of their binding partner (18).

The balance of Runx3 and GATA3 regulates the relative expression levels of IFN-γ and IL-4 in TCR-stimulated $CD4^+$ cells

To determine the effect of modulating the relative amounts of Runx3 and GATA3 on IFN-γ and IL-4 expression, isolated splenic $CD4^+$ cells were stimulated with TCR and cultured under nonskewed conditions. The cells were then doubly infected by two retroviruses (Fig. 5), one encoding bicistronic *Runx3* and *GFP* and the second encoding *GATA3* and rat *CD2*. GFP and rat CD2 were used as markers for monitoring Runx3 and GATA3 expression, respectively. In noninfected cells, the IFN-γ- and IL-4-positive fractions were present in a 1:1 ratio (11 and 10%, respectively; Fig. 5, *lower left*). The overexpression of GATA3 decreased the ratio of IFN-γ and IL-4 to 0.4 (9 and 23%, respectively; *upper left*), whereas the overexpression of Runx3 increased the ratio of IFN-γ and IL-4 to 4.2 (23 and 5%, respectively; *lower right*). In doubly infected cells, the ratio of IFN-γ to IL-4 reverted to 1.1 (17 and 15%, respectively; Fig. 5, *upper right*). These results indicated that in TCR-stimulated cells, Runx3 and GATA3 can attenuate each other's effect on the expression of IFN-γ and IL-4 (See supplemental Fig. 2 in which similar experiments as Fig. 5 was performed but under Th1 and Th2 conditions as well. Mutual countering effects of Runx3 and GATA3 were confirmed again.).

Transgenic expression of Runx3 can activate IFN-γ and silence IL-4 in cultured $CD4^+$ cells

To determine whether the effects we were observing in vitro in cultured $CD4^+$ cells were also true in vivo, we analyzed cells from mice that expressed an *Lck*-driven *Runx3* transgene (15). Fig. 1

Downloaded from www.jimmunol.org on February 23, 2010

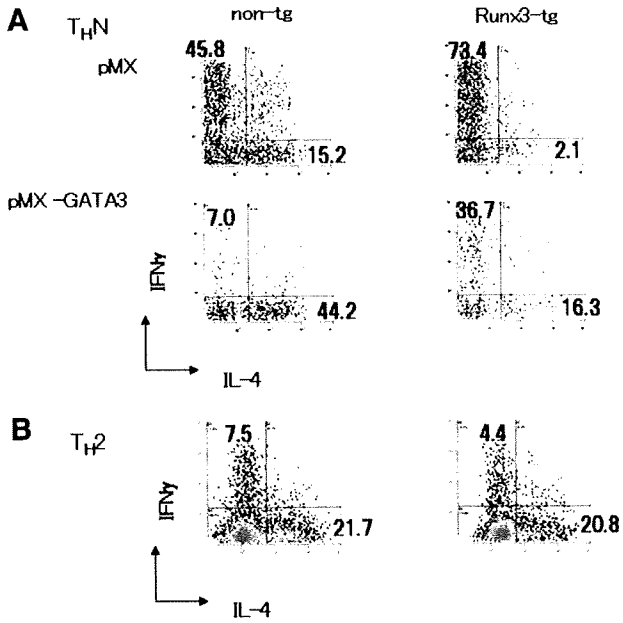

FIGURE 6. Effect of transgenic (tg) *Runx3* expression on IFN-γ and IL-4 expression. $CD4^+$ cells were isolated from the spleens of nontransgenic (non-tg) and *Runx3*-transgenic mice, stimulated with TCR, and then infected by a retrovirus carrying pMX-GFP or pMX-GATA3-IRES-GFP. After 7 days in culture under nonskewing (*A*) or Th2 (*B*) conditions, the cells were re-stimulated and then analyzed by intracellular staining for IFN-γ and IL-4, followed by flow cytometry. The fluorescence intensity of IFN-γ and IL-4 in the GFP-positive population is displayed. Numbers represent the percentages of cells in each quadrant. The GATA3:Runx3 protein ratio in Th2-conditioned *Runx3*-transgenic cells was >1.0 (actually, it was 0.7:0.3 = 2.3 in Fig. 1, *lane 12*) as in the case of Th2-conditioned nontransgenic cells (1.7:0.5 = 3.4 in Fig. 1, *lane 9*). Therefore, it may not be unreasonable that Th2-conditioned *Runx3*-transgenic cells showed a Th2-like phenotype (*B*). In contrast, in Fig. 2, retrovirally introduced Runx3 overexpressing cells for which the Runx3:GATA3 ratio was 3.5:1.0 = 3.5 exhibited a Th1 phenotype even under a Th2 condition.

shows the Runx expression profile of isolated *Runx3*-transgenic $CD4^+$ cells that were stimulated through the TCR with anti-TCRβ Abs. The level of Runx3 in transgenic ThN cells was 1.5-fold higher than that in nontransgenic ThN cells and rather equivalent to that in nontransgenic Th1 cells (Fig. 1, compare *lanes 7, 8,* and *10*). To determine whether *Runx3*-transgenic cells under nonskewed conditions also mimicked nontransgenic Th1 cells in terms of IFN-γ and IL-4 expression, we analyzed intracellular IFN-γ and IL-4 levels by flow cytometry. As seen in Fig. 6*A*, under nonskewed conditions, *Runx3*-transgenic cells exhibited enhanced IFN-γ expression (73%) and marked repression of IL-4 expression (2%) as compared with nontransgenic cells (Transcription of Th2-type cytokines including *IL-4, IL-5,* and *IL-13* were substantially reduced in *Runx3*-transgenic ThN cells. See supplemental Fig. 3.).

We next examined whether the magnitude of IFN-γ and IL-4 expression in *Runx3*-transgenic cells was also responsive to the balance of Runx3 and GATA3, as observed in wild-type $CD4^+$ cells. The introduction of *GATA3* into *Runx3*-transgenic cells resulted in a decrease in the percentage of IFN-γ-positive cells (37%), and an increase in the percentage of IL-4-positive cells (16%) as compared with the nonintroduction of *GATA3* (Fig. 6*A*). However, *Runx3*-transgenic cells remained to exhibit a Th2-like expression profile of IFN-γ and IL-4 even when cultured under Th2-permissive conditions (Fig. 6*B*; there was no virus infection in this panel). The result in Fig. 6*B* was in agreement with the relative

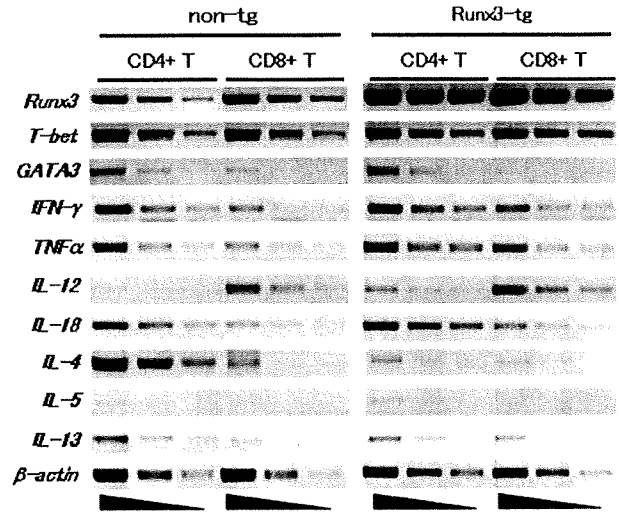

FIGURE 7. Cytokine expression profiles in naive *Runx3*-transgenic (tg) $CD4^+$ cells. RNA was prepared from naive $CD4^+$ and $CD8^+$ cells from nontransgenic (non-tg) and *Runx3*-transgenic mouse spleens. Increasing amounts of cDNA were used for semiquantitative RT-PCR of cytokine gene transcripts under nonsaturating conditions. β-Actin was analyzed as a control.

expression levels of Runx3 and GATA3 proteins as detected in Fig. 1 (see the legend of Fig. 6 for detailed discussion on the Runx3:GATA3 or GATA3:Runx3 ratios).

These results collectively indicated that transgenic expression of *Runx3* can activate IFN-γ expression and silence IL-4 expression, similar to its effects in vitro in cultured $CD4^+$ cells.

Runx3-transgenic naive $CD4^+$ cells are biased toward a Th1 phenotype

When $CD4^+$ cells were isolated from *Runx3*-transgenic spleens and analyzed immediately by immunoblot, an observed Runx expression profile was the same as that seen in Fig. 1, *lane 10* (data not shown). This suggests that *Runx3*-transgenic naive $CD4^+$ cells have already acquired a Th1 phenotype. To test this hypothesis, we compared the expression profiles of various Th1- and Th2-specific genes in naive $CD4^+$ cells that were isolated from *Runx3*-transgenic and nontransgenic mice by semiquantitative RT-PCR analysis (Fig. 7). As a control, we also examined gene expression in $CD8^+$ cells in parallel. As compared with nontransgenic cells, *Runx3*-transgenic cells expressed an excessive amount of *Runx3* transcript, however, the levels of *T-bet* and *GATA3* transcripts were unaffected. The levels of several Th1-type cytokine transcripts (*IFN-γ*, TN*Fα*, *IL-12*, and *IL-18*) were uniformly increased in *Runx3*-transgenic cells. In contrast, the levels of Th2-type cytokine transcripts (*IL-4* and *IL-13*) were decreased in transgenic cells. These results indicated that *Runx3*-transgenic $CD4^+$ cells are prone to a Th1 phenotype, even in the absence of TCR-stimulation.

Th1-specific immunological responses in Runx3-transgenic mice

We next examined the Th1- and Th2-mediated immunological responses of *Runx3*-transgenic mice. Mice were immunized with OVA mixed with CFA, and serum Ab titers were measured (Fig. 8*A*). After a second boosting injection (day 28), the titers of IgG2a and IgG2b were significantly higher in *Runx3*-transgenic mice than in nontransgenic mice. IgG2a and IgG2b are the Ig subclasses the production of which depends on a Th1 response. We also examined mice that were immunized with OVA mixed with aluminum hydroxide (Fig. 8*B*). OVA mixed with aluminum hydroxide is a form of Ag that tends to trigger the Th2-dependent production of

Downloaded from www.jimmunol.org on February 23, 2010